Chapter 3   Ground Survey

3.1   Drilling, Laboratory Tests

The outline of the lithologic structure in Yerevan can be understood by the geological maps and the collected drilling database, which contains 5,094 logs; however, the data concerning the S wave velocity for the amplification analysis and the soil properties for the liquefaction analysis are not enough. To collect these data, 10 drillings were newly conducted in Yerevan and several tests were conducted using these boreholes. The quantities of the tests are shown in Table 3.1-1.

Table 3.1-1   Quantities of Tests

Category	Quantities
Drilling	30m x 10
Groundwater Level Measurement	10
Standard Penetration Test	129
Disturbed Soil Sampling	116
Laboratory Test	116

The drilling points are mainly set to the area where the Quaternary deposits cover because it is effective for the amplification of the earthquake motion by the ground and liquefaction potential. The geologic condition of Yerevan was estimated as follows from the existing information. The rock layer may be shallow in the northern area and the soft soils cover the southern area. Therefore, the selected newly boring points locate in the south of Yerevan city (Figure 3.1-1). The surface soils of each drilling points are shown in Table 3.1-1. The drilling logs are shown in Data Book. The example of drilling log is shown in Figure 3.1-1.
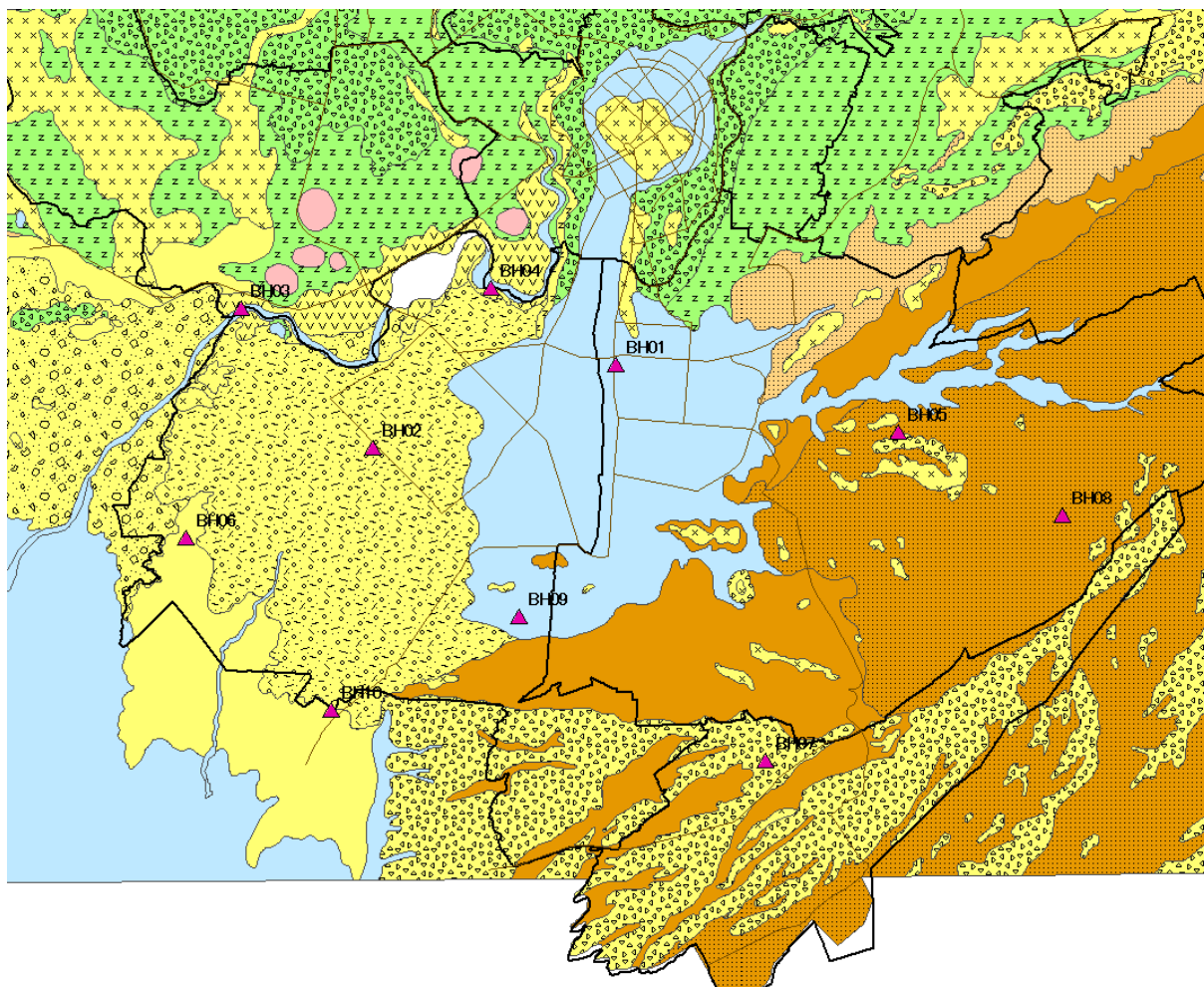
Figure 3.1-1   Location of drilling points

Table 3.1-2   Surface geology of the drilling points

Quaternary layer		
Symbol	Age	No. of Drilling Point
apQ42	Modern Section (the upper part)	3
apQ41	Modern Section (the lower part)	1, 9
apQ2-3chr	Middle-to-Upper Quaternary Sections (the lower part)	2
apQ3ar	Upper Quaternary Section (the lower part)	4
laQ1-2	Lower-to-Middle Quaternary Sections	6, 10
Q1nb1	Lower Quaternary Section (the lower part)	7
Tertiary rocks		
Pg3sh3	Lower-Middle Oligocene	5, 8

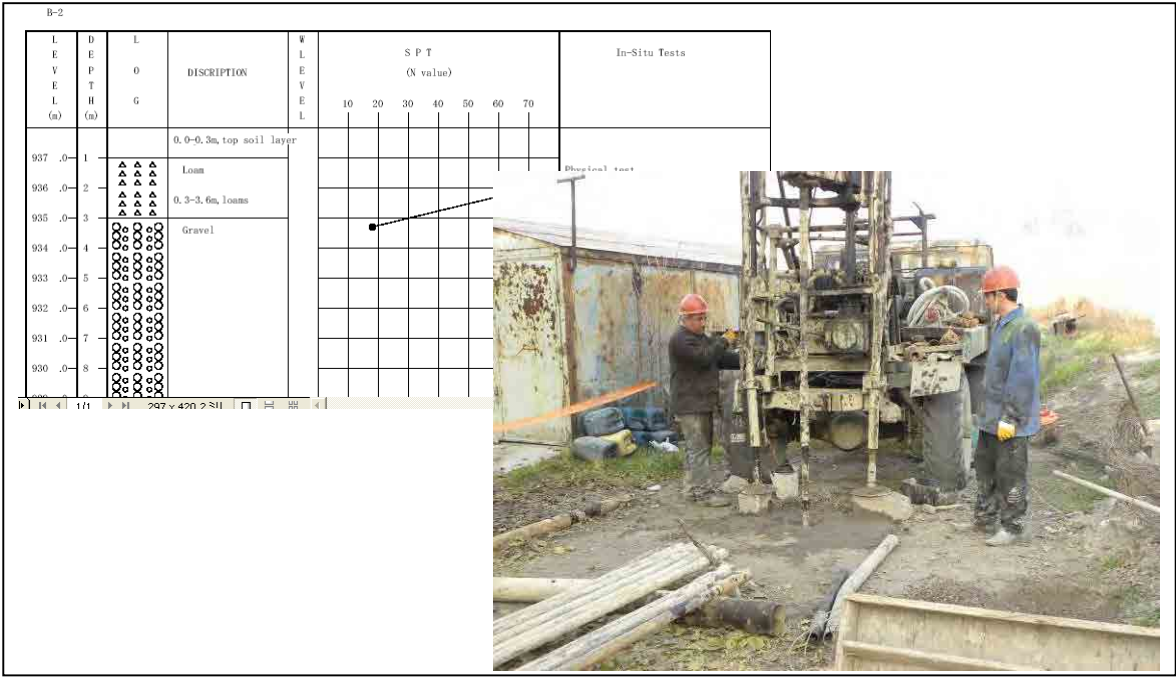Figure 3.1-2   Sample of drilling log and the drilling condition

3.2 PS Logging

PS logging is carried out at the 10 newly conducted drilling points using the borehole. PS logging is the geophysical survey method to get the S wave velocity of the soil layers receiving the surface generated waves in the borehole using the borehole receiver. The S wave velocity is calculated by dividing the distance between the wave generator to the receiver by the time difference between generation and receiving. As the S wave is shear wave, a big wooden plank is placed on the ground surface to generate and the end is hit horizontally by the iron hammer. Both ends are hit and the S wave can be detected by pointing the phase which shows inversely by two hits. Figure 3.2-1 shows the sample of observed S wave form by two sides of the plank and the condition of S wave generation. The results of PS logging are shown in Data Book.
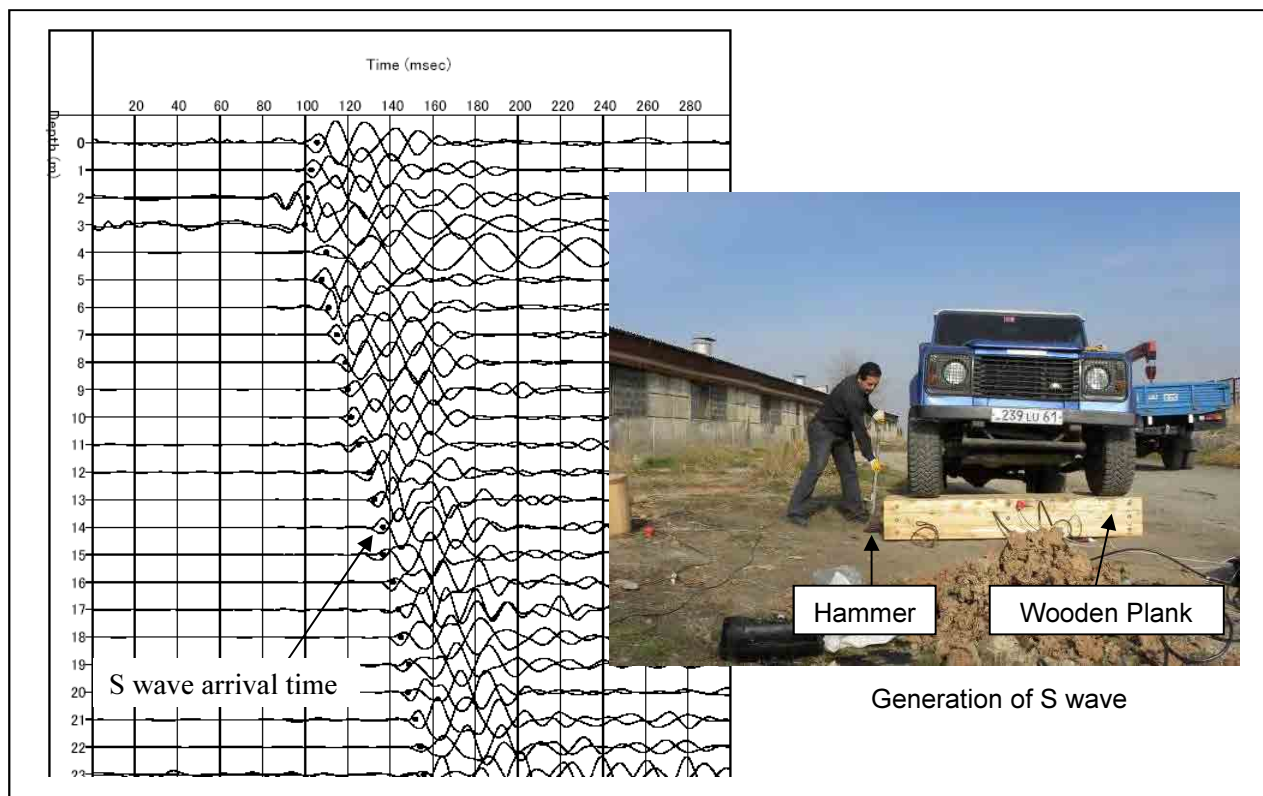
Figure 3.2-1   Sample of observed S wave and the condition of S wave generation

3.3   Surface Wave Exploration

Surface wave exploration is carried out at the 60 points in Yerevan city (Figure 3.3-1). Surface wave exploration is the geophysical survey method to get the S wave velocity structure of the soil layers using the artificially generated surface wave or the natural microtremor. The surface wave is observed by the several geophones at ground surface simultaneously and analysed. In this study, 24 geophones are placed in L-shape in 2m interval and observed the microtremor (Figure 3.3-2). This method is the in-direct method using the observed waves at ground surface. The S wave structure in the ground is obtained after processing and analysis. Therefore the accuracy is lower than the PS logging, which is the direct method using the observed S wave in the ground; however it has the advantage in the cost and readiness because this method don't needs borehole.

An example of comparison between S wave structure model by surface wave exploration method and PS logging at same place is shown in Figure 3.3-3. The obtained S wave structure by surface wave exploration method is compatible to the result by PS logging. All the comparison between 10 PS logging and the results by surface wave exploration method at same places show agreement. The usefulness of the surface wave exploration method is confirmed at least in the ground condition like Yerevan. The results are shown in Data Book.
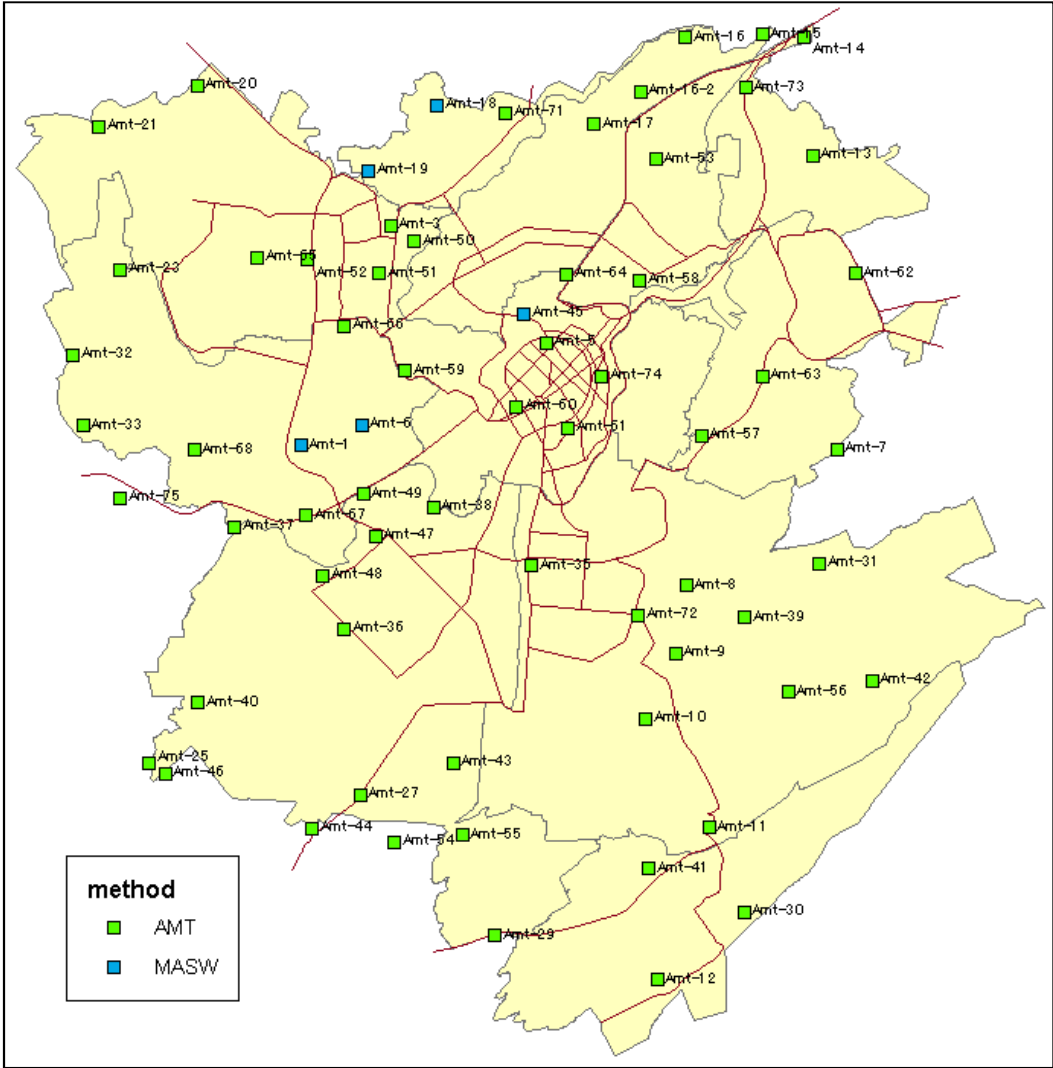
Figure 3.3-1   Location of Surface wave exploration and microtremor survey points

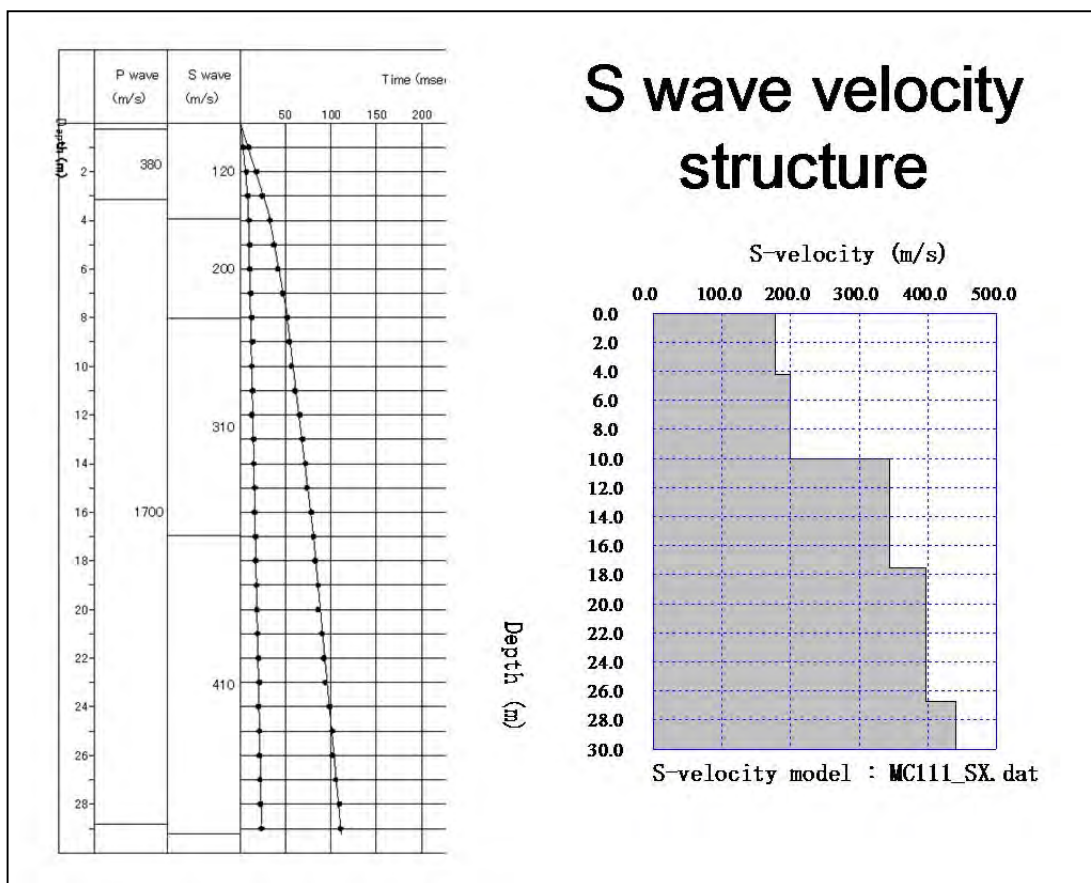Figure 3.3-2   L-shape setting of geophones for surface wave exploration

Figure 3.3-3   Comparison between the result by surface wave exploration (right)
and PS logging (left)

3.4 Microtremor Survey

Microtremor survey is carried out at the same places to the surface wave exploration points (Figure 3.3-1). The mircrotremor is the phenomenon of very small vibration of the ground surface as a result of a complex stacking process of various waves propagating from remote man-made vibration sources caused by traffic systems or machinery in industrial plants, and from natural vibration caused by tidal or volcanic activities. Microtremor can be observed anywhere on or below the ground surface.

The observed microtremor reflects the physical properties of the ground over the clear contrast of S wave velocity. The spectrum of the observed microtremor wave indicates the S wave velocity structure. The H/V (Horizontal/Vertical) spectral ratio sometimes show better result than the horizontal spectra and used widely. The H/V spectrum are calculated and used to confirm the S wave velocity structure by surface wave exploration method in this study. An example of the result is shown in Figure 3.4-1. All the results are shown in Data Book.
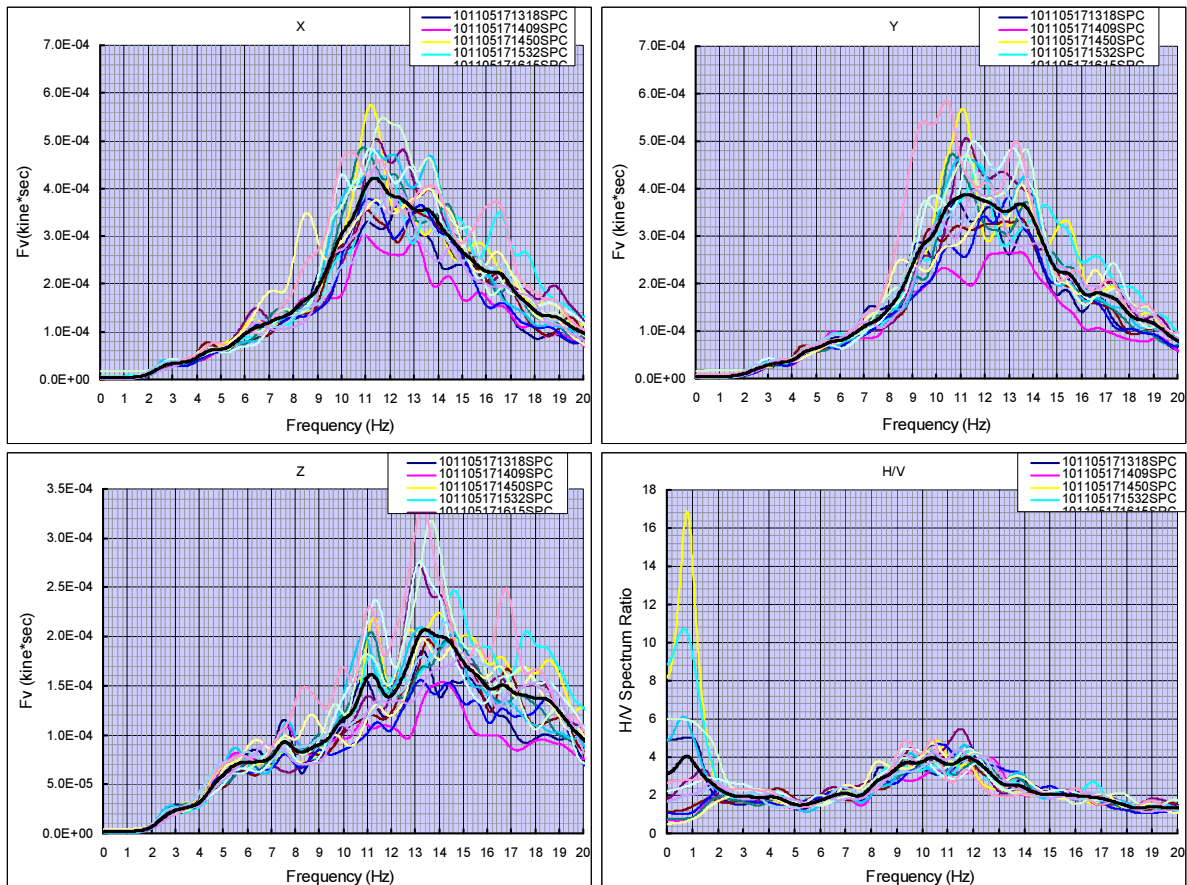
Figure 3.4-1   Example of the spectrum by microtremor survey

3.5 Surface Geology Mapping

Studies of the geological structure, tectonics and history of geological evolution of the Near-Yerevan region have been conducted over many years by different organizations, including the Institute of Geological Sciences, Divisions of the Geology Department, and other institutes, as well as by individual researchers – A. Aslanyan, A. Gabriyelyan, K. Paffenholtz, R. Arakelyan, S. Arzoumanyan, A. Nazaryan and other.   In relation to seismic micro-zoning activities carried out in 1990, Yu. Sayadyan and E. Kharazyan prepared a Summary Geological Map of the Yerevan City at the scale of 1:10,000 (Sayadyan and Kharazyan, 1990). In 1993, E. Kharazyan prepared the 1:25,000 Geology Map of Yerevan and Near-Yerevan Region. In 2004, "Georisk" prepared the 1:10,000 Geological map of the Yerevan City in GIS format.

As "Georisk" owns accumulated data and experienced geologist, the study team contracted with Georisk for the SUBSURFACE GEOLOGICAL MAP GENERATION. The contract includes collection of existing data, collection and analysis of new borehole data and supplementary field survey for compiling subsurface geological map to be used ground type modeling for seismic response analysis and landslide assessment.

Previous geological study and existing Geological maps are published by Sayadyan and Kharazyan (1990), Kharazyan (1993) and "Georisk" scientific research company (2004). Two previous Geological Maps are shown as following Figure 3.5-1 and Figure 3.5-2.
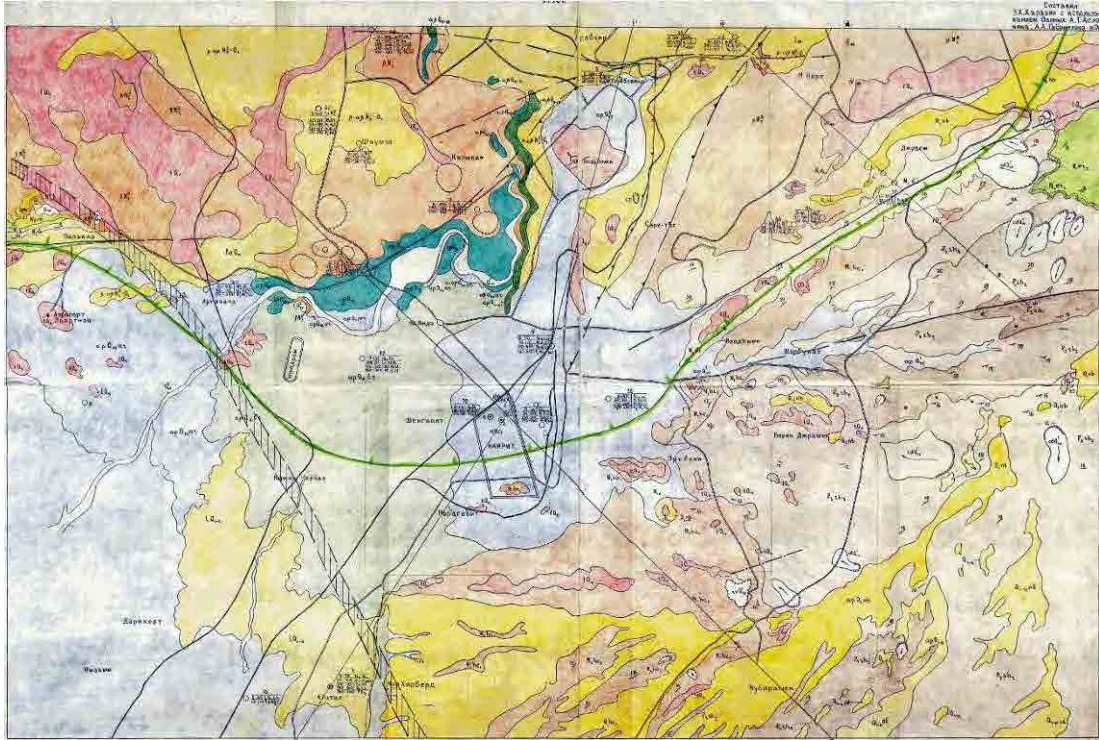
Figure 3.5-1   Geological Map (E.Kharazyan et al.1993)The scale 1:25,000
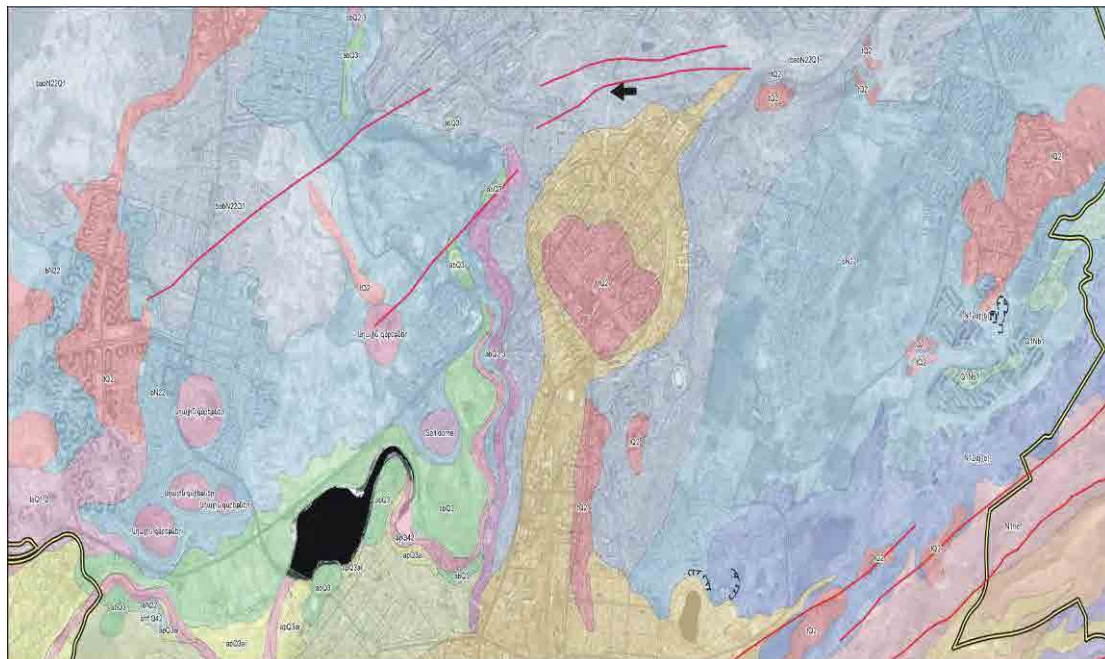
Figure 3.5-2   Geological Map of scale 1:10,000 (Georisk 2004)

The subsurface geological map of this project is utilized for ground type modeling, so vertical geological structure was emphasized. The 1:25,000 and 1:10,000 subsurface geological maps were generated by compilation of existing data and new borehole data done by this project. For understanding detail geological structure, two kinds of geological cross sections are generated with the report. One is 8 cross sections with horizontal scale 1:10,000 and vertical scale 1:4,000 for whole city area, and the other is 6 cross sections with horizontal scale 1:10,000 and vertical scale 1:1,000 for low land area. These geological data are summarized by GIS, which are submitted simultaneously. The examples of them are shown in Figure 3.5-3 to Figure 3.5-6.
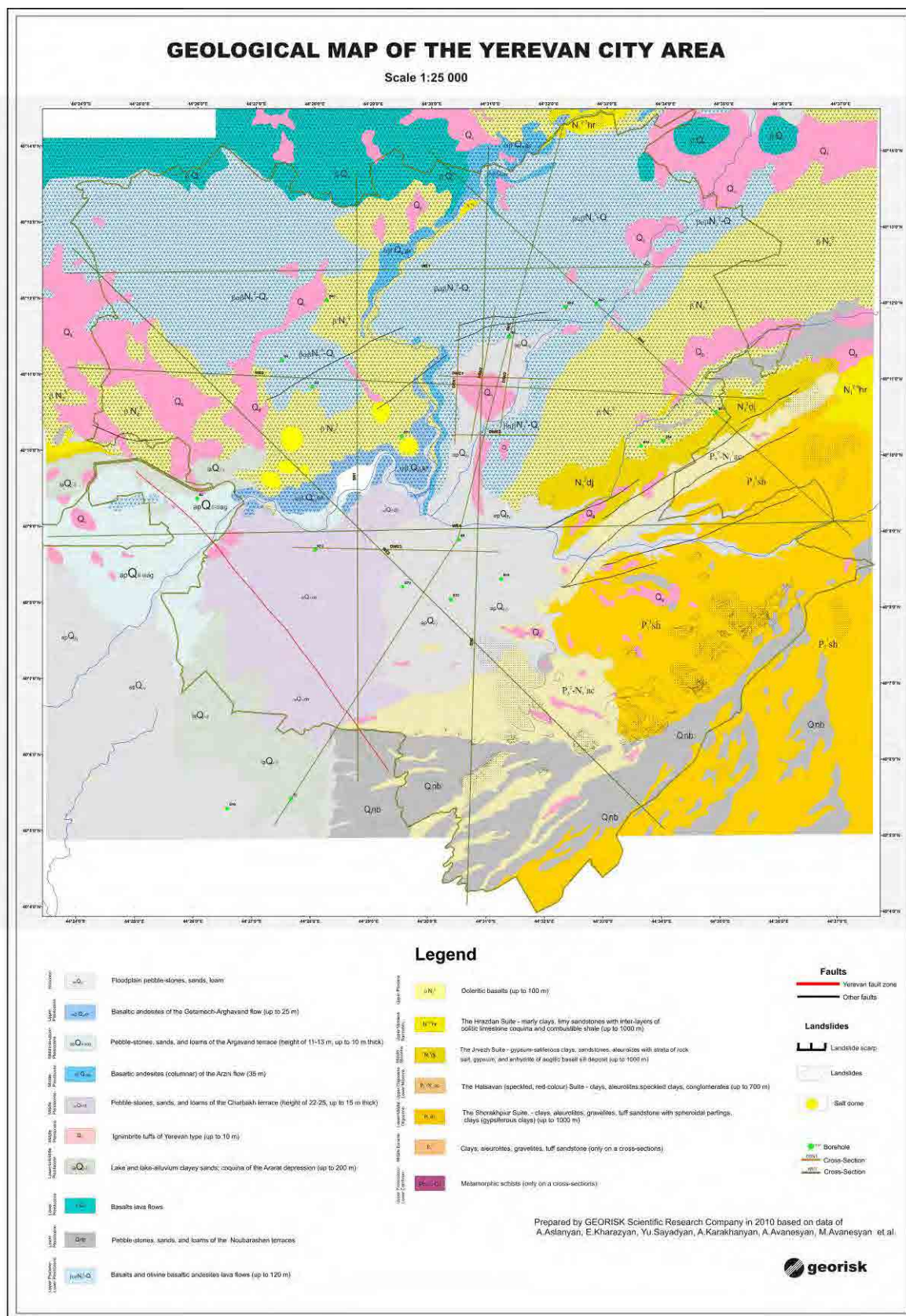
Figure 3.5-3   Geological map of the Yerevan City area
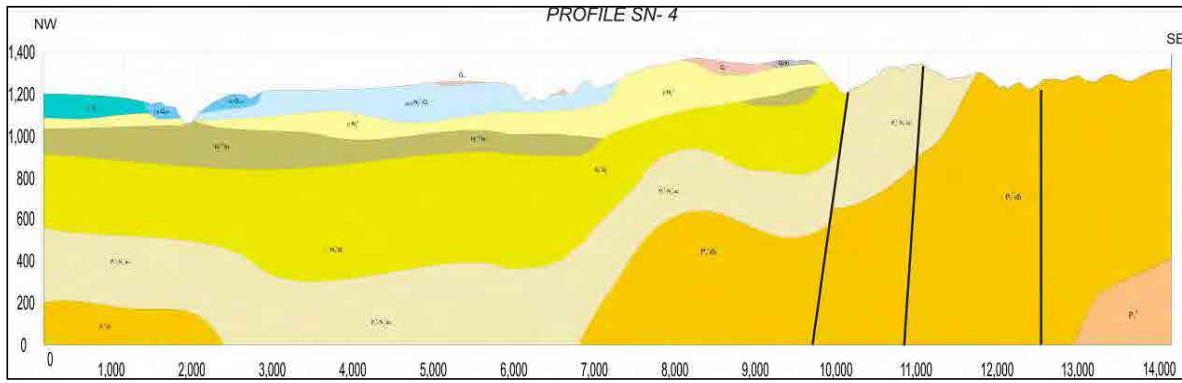
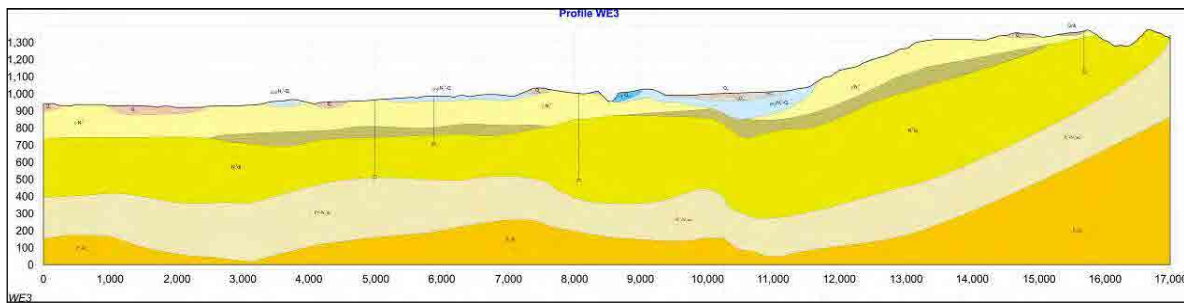Figure 3.5-4   An example of Geological Cross Sections (SN direction No.4）

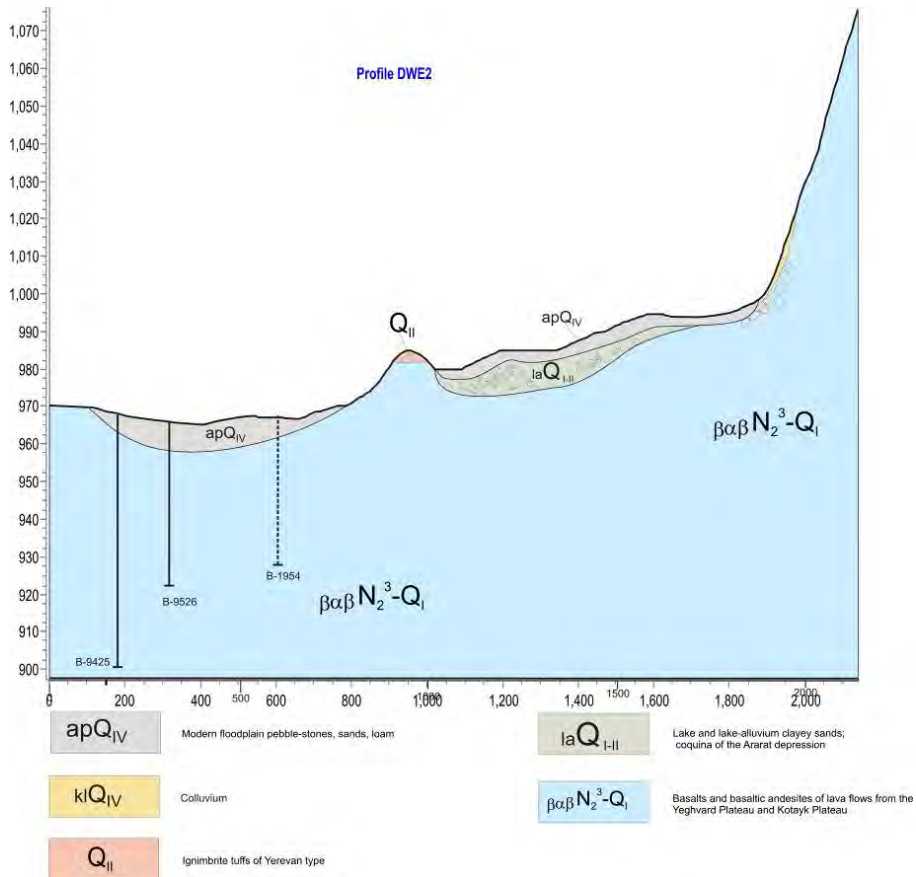Figure 3.5-5   An example of Geological Cross Sections (EW direction No.3）

Figure 3.5-6   An example of Detailed Geological Cross Sections (Detail EW direction No.2)

3-11

Table 3.5-1   Detail stratigraphy of the territory of Yerevan city

Geological Ages			Names of layers	Symbols	Description
Quaternary			Holocene / Flood plain deposits	apQ_{IV}	Floodplain pebble-stones, sands, loam
			Upper Pleistocene / Getamech-Argavand lava flow	$\alpha\beta Q_{III}$ ga	Basaltic andesites of the Getamech- Argavand flow (up to 25 m)
			Middle to Upper Pleistocene / Arghavand terrace deposits	$apQ_{II\text{-}III}$ ag	Pebble-stones, sands, and loams of the Argavand terrace (height of 11-13 m, up to 10 m thick)
			Middle Pleistocene / Arzni lava flow	$\alpha\beta Q_{II}$ ar	Basaltic and sites (columnar) of the Arzni flow (35 m)
			Middle Pleistocene / Charbakh terrace deposits	apQ_{II} ch	Pebble-stones, sands, and loams of the Charbakh terrace (height of 22-25 m, up to 15 m thick)
			Middle Pleistocene / Tuff of Yerevan type	Q_{II}	Ignimbrite tuffs of Yerevan type (up to 10 m)
			Lower to Middle Pleistocene / Ararat suite	$laQ_{I\text{-}II}$	Lacustrine and alluvium clayey sands; coquina of the Ararat depression (up to 200 m)
			Lower Pleistocene / Yeghvard plateau lava and Kotayk plateau lava	βQ_I	Basalts lava flow
			Lower Pleistocene / Noubarasheu terrace deposits	Q_I nb	Pebble-stones, sand, and loam (height of 180 m, up to 70 m thick)
Tertiary	Neogene		Upper Pliocene to Lower Pleistocene / Yeghvard plateau lava and Kotayk plateau lava	$\beta\text{-}\alpha\beta N_2^{\ 3}\text{-}Q_I$	Basalts and olivin basaltic andesites lava flow (up to 120 m)
			Upper Pliocene / Doleritic basalts	$\beta N_2^{\ 3}$	Doleritic basalts (up to 100 m)
			Upper Miocene Sarmatian Part / The Hrazdan suite	$N_1^{\ 2\text{-}3}$hr	Marly clay, limy sandstone with inter-layers of oolitic limestone coquina and combustible shale
			Middle Miocene / The Jrvezh suite	$N_1^{\ 2}$ dj	Gypsum-saliferous clay, sandstone, aleurolite with strata of rock salt, gypsum, and anhydrite of augitic basalt sill deposits(up to 1000m)
	Paleogene		Upper Oligocene to Lower Miocene / The Hatsavan suite	$P_3^{\ 2}\text{-}N_1^{\ 1}$ ac	Clay, aleurolite, speckled clay, conglomerate (up to 700m)
			Lower to Middle Oligocene / The Shorakhpiur suite	$P_3^{\ 1}$sh	Clay, aleurolite, gravelite, tuff sandstone with spheroidal partings, clay(gypsiferous clay) (up to 1000m)
			Middle Eocene / Clay, aleurolite, gravelite, tuff sandstone	$P_2^{\ 2}$	Clay, aleurolite, gravelite, tuff sandstone (only in the cross sections)
Proterozoic to Paleozoic			Upper Proterozoic to Lower Cambrian / Metamorphic basement	$Pr_3\text{-}C_1$	Metamorphic schist (only in the cross sections)
			Rock Salt		

Geology of the territory of Yerevan city is as follows.

(1) Paleogene rocks and sediments

The volcanogenic-debris Voghjaberd Suite (Meotian-Pontian age) was drilled by boreholes under the lava of the Kotayk volcanic plateau and Yeghvard volcanic plateau. It is exposed in the Jrvezh ricer gorge region and builds the Voghjaberd mountain range. The suite is rather irregularly built of

distributed effusive, pyroclastic and fragmental materials, and is represented by tuff breccias, tuff conglomerates, tuff sandstone, tuff, and pumice-ashy units.

The south-eastern outskirts of the city area are located within the Shorakhpiur-Noubarashen sloping plain, the principal structural unit of which is the Shorakhpiur   anticlinal fold. Approximately, the axis of this fold runs along the line linking the villages of Shorakhpiur and Ghehadir (Kotayk region). The rocks of the Shorakhpiur suite (P_3^1sh) which exposed that area, are related to the Early Eocene-Oligocene and are represented by aleurolites, tuff sandstone, sandstone, and conglomerates with inter-layers of gypsiferous clays and lenses of reef limestone.

(2) Neogene rocks and sediments

Directly south of the Nork-Marash district and the Jrvezh Village, it is possible to observe exposures of the Early-Middle Miocene rocks that are located above the Shorakhpiur suite (P_3^1sh)   by stratigraphy; they are related to the Hatsavan suite (P_3^2-N_1^1ac) composed of unconsolidated conglomerates, sandstones, red-colored clays, aleurolites, and to the Jrvezh suite (N_1^2dj) that is developed extensively over the lava flow in Kanaker area of Kotayk volcanic plateau and includes cloddy sandy clays, sandstones, and argillites with strata and inter-layers of rock salt and gypsum.

Exposures observed in this region demonstrate that the mentioned suite underlies, and alternates with the Sarmatian fresh-water and marine clayey sediments of the Hrazdan Suite (N_1^{2-3}hr), which is also known to have outcrops in other parts of the described area, namely, within the site between Arzni Resort and the Kanaker Hydro Power Plant and in the Parakar Village region. Besides, these deposits were drilled by boreholes almost within the entire Yerevan Depression.

The surface of dolerite basalts（βN_2^3）in the Kotayk volcanic plateau and Yeghvard volcanic plateau were overlain with a few flows of single extensive cover of the Late Pliocene-Early Quaternary basalts, and olivine basaltic andesites（β-$\alpha\beta N_2^3$-Q_1）

(3) Pleistocene of Quaternary rocks and sediments

In the southern and eastern outskirts of Yerevan, Nubarashen and Nor Kharberd,   the complexes of the Tertiary rocks are overlain by coarse-fragmental pebble formations with filling of gravel and sand; these are known as the Nubarashen terrace deposits (Q_1nb) of an Early Quaternary age. The sediments are derived from Dzoraghbyur mountains and old volcanoes in Kotayk region.

Kotayk volcanic plateau and Yeghvard volcanic plateau are widely covered by basalt and basaltic andesite（ βQ_1 and β-$\alpha\beta N_2^3$-Q_1）, which developed a thick (up to 150 m) cover over relatively even surface of the dolerite basalts, olivine basaltic andesites and others.

The lower part in the section of volcanic formations of the Kotayk volcanic plateau and Yeghvard volcanic plateau includes dense, porous, grey and dark-grey-colored dolerite basalts（βN_2^3）of a Late Pliocene age, which have the average thickness of 20 to 30 m. The mentioned basalts formed a vast polygenic cover, consisting of a series of single-episode lava effusions, which, in fact, did created the lava massif of the Kotayk volcanic plateau and Yeghvard volcanic plateau.   Their structure is clearly

observed in the gorges of the Hrazdan and Jrvezh rivers, as well as within the exposures located directly in the city limits.

The Arzni lava flow ($\alpha\beta Q_{II}ar$) of breccia-shaped basaltic andesite, which can be traced along both sides of the Hrazdan river gorge up to the Kanakeravan in Kotayk region, as well as the Yerevan flow of columnar quartz-bearing basaltic andesite, are related to this series.

Along the west bank of the Hrazdan River, it is possible to trace individual fragments of the Ghetamech-Argavand lava flow ($\alpha\beta Q_{III}ga$), the thickness of which varies in the range of 8-25 m. These young columnar basaltic andesites occur on the Argavand pebble terrace and, along with the latter, are dated to the Late Pleistocene. Individual fragments are traced in the Yerevan Lake area, near the Karmir Blour Fortress(west of Erebuni district) and Argavand village(Ararat region), where the termination (the tongue) of the lava flow is clearly manifested.

The bottom of the Ararat accumulation plain is filled with sedimentary formations of the Early-Middle Quaternary Ararat Suite(laQ_{I-II}), represented by lake and lake-alluvial sediments. The thickness of the sediments ranges up to 180-200 m; in the upper part of the section, clayey sediments are followed by gravel and pebble lake-and-alluvial formations.

Argavand terrace of the Hrazdan river is developed in the suburb district of Argavand village, where it has a relative height of 11-13 m; the terrace is built of well-smoothened pebble and has the filling material of gravel-sand-clay composition, named Argavand terrace deposit ($apQ_{II-III}ag$).

(4) Holocene (Recent sediments)

Recent sediments within the central and southern parts of the territory of Yerevan city are represented by channel deposits (apQ_{IV}) of the Hrazdan river, Jrvezh river, Getar river, Dzoraghbyur river, and Shorakhpiur river. Channel and floodplain facies of the listed rivers, including pebble, sand, loamy sand and clays, are well developed in their downstream courses at the entering to the Ararat accumulation plain.

3.6 Landslide Survey

3.6.1 Flowchart of the study

The flow of the landslide study as shown in Figure 3.6-1.

Information on landslides in the territory of Yerevan city was provided form "Georisk". Furthermore, the study team had the results of previous project, "The study on landslide disaster management in the Republic of Armenia". Although, those data are important for this project, many changes of the state of landslides after those previous studies were found by the preliminary field investigation. For generation of new landslide distribution map, satellite image of ALOS taken in 2008 were used for photo interpretation.

After satellite photo interpretation, landslide micro landforms, such as, main scarps, cracks, steps, depressions and mounds, and damage to houses, buildings and infrastructures were observed in the field

for revising the results of satellite photo interpretation. Based on the revision and the damage investigation, this information was arranged by GIS.

```
┌─────────────────────────────────────────┐
│   Collection of Existing Data on Landslides   │
└─────────────────────────────────────────┘
                    │
┌─────────────────────────────────────────┐
│  Preliminary Landslide Mapping by GEORISK    │
└─────────────────────────────────────────┘
                    │
┌─────────────────────────────────────────┐
│      Satellite Image Interpretation          │
└─────────────────────────────────────────┘
                    │
┌─────────────────────────────────────────┐
│   Surface Anomaly and Damage Survey on Site   │
└─────────────────────────────────────────┘
                    │
┌─────────────────────────────────────────┐
│   Amendment of Preliminary Landslide Map      │
└─────────────────────────────────────────┘
                    │
┌─────────────────────────────────────────┐
│    Landslide Hazard and Risk Assessment       │
└─────────────────────────────────────────┘
                    │
┌─────────────────────────────────────────┐
│ Slope Classification and Landslide and Rock Fall Potential Assessment │
└─────────────────────────────────────────┘
                    │
┌─────────────────────────────────────────┐
│    Landslide Hazard and Risk Mapping by GIS   │
└─────────────────────────────────────────┘
                    │
┌─────────────────────────────────────────┐
│ Propose for Slope Hazards Countermeasures in case of Earthquake │
└─────────────────────────────────────────┘
```
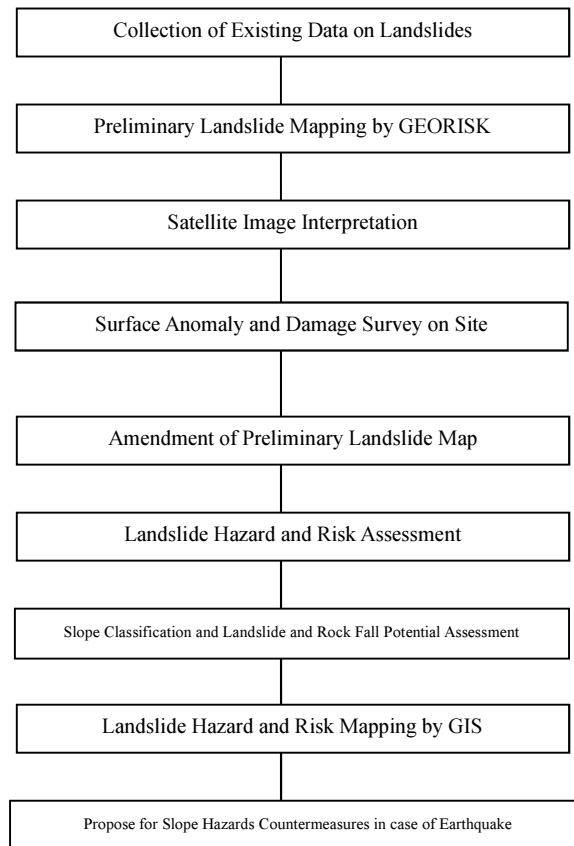
Figure 3.6-1   Flow of the landslide study

3.6.2   Landslides distribution

Landslides are distributed densely in the southern and eastern sloping plain in the territory of Yerevan city. The size of the landslides ranges from 100m long and 0.5ha which are small ones to 1km long and 1.5km^2 wide which are large ones. Large landslides exist especially in the southern and eastern of Erebuni district and Nubarashen district.

Mainly, landslides are developed in areas that have clayey soils in their geological-lithological section, or where soil stratum diversities capable of generating landslide planes are present in the composition of the suite. By the main geological-tectonic factor and the geographic location, the landslides and landslide hazard areas can be subdivided into the following three groups:

1. Shorakhpiur-Nubarashen (Sovetashen) Landslide Group.
2. Jrvezh Landslide Group
3. Hrazdan Landslide Group

Landslides in Group 1 "Shorakhpiur- Nubarashen (Sovetashen) Landslide Group" spread from the south-eastern slopes of the Nork volcanic upland to the high Nubarashen terrace of the Arax river. This

group includes landslides that developed in the region of the Yerevan by-pass road, as well as the landslides of the Sovetashen Hospital Complex, Sovetashen cemetery, garbage collector, Bardzrashen village, Sovetashen poultry farm, Sovetashen upland, Shorakhpiur village vicinity, Sovetashen alluvial terrace, and a few other landslides. As a rule, the listed landslides start to develop at slope base and then spread upward over the slope. Underground waters in the form of springs are observed in many landslide tongue areas.

Landslides spread the geological areas of the speckled clay, gypsum and salt-bearing soils, and whitish rocks of the Paleogene and Neogene.

Landslides in Group 2 "Jrvezh Landslide Group" are related only to the exposures of gypsiferous clays that are exposing within a narrow strip on the southern and southeastern slopes of the Kotayk volcanic plateau, from the Vardavar lake up to the Jrvezh Village (Kotayk region) area. Pliocene-age dolerite basalts are bedded on the washed-out and uneven surface of the clays; the thickness of the basalts varies in the range from few to tens of meters. The clays that serve as sliding plane are, as a rule, abundantly moist and in plastic flowable condition.

Landslides in Group 3 "Hrazdan Landslide Group", are exist mainly on the right and left banks of Hrazdan river gorge, and are associated with sites of exposed clay and marly rocks, on which thick basaltic lavas are bedded and the boundary of which is always water-saturated. Therefore, not only the basalts and basaltic andesite, but also the residual and creeping units, covering the clayey suite, are capable of landslide.
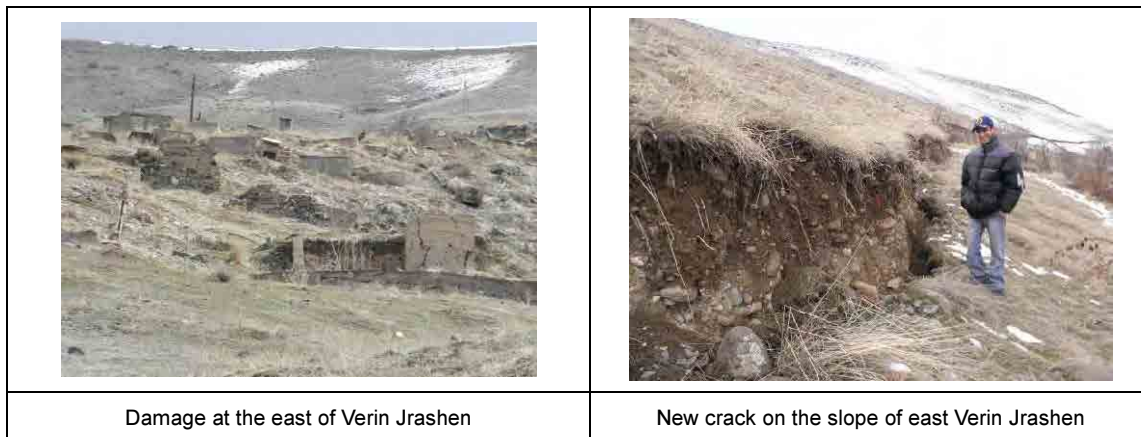
Landslides on the down Sovetashen Hospital Complex	Damage at Nor Kharberd

Damage at the east of Verin Jrashen	New crack on the slope of east Verin Jrashen

Figure 3.6-2   Landslides and damage

3.7 Active Fault Survey

3.7.1 Purpose and Contents of Active Fault Survaey

It is necessary to consider the following items in order to set up scenario earthquakes in Yerevan City.

1) Detailed location of active faults

2) Fault type (strike-slip, reverse, normal fault), length, dip

3) Probability of future earthquake occurrence inferred from faulting history

4) Expective magnitude

The contents of active fault mapping are satellite photo interpretation, field survey, trench investigation, and radiocarbon dating. The active fault maps after Philip et al. (2001) and Georisk report are available in Armenia. The validity of these maps is discussed based on the active fault mapping.

The faulting history of active faults is studied by the analysis of documents on the historic earthquakes. However, even if there are some documents on the damage of seismic event, the active fault as a seismic source cannot be specified in many cases. So trench investigation is necessary in order to detect the time of paleo-earthquakes.

ALOS images acquired by Japanese satellite "DAICHI" and CORONA images were used for satellite photo interpretation. CORONA images cover almost whole Armenia and ALOS images are limited around Yerevan City. The ID number and photographed date are shown in Table 3.7-1 and Table 3.7-2.

Table 3.7-1   ID number and photographed date of ALOS images

Forward	Backward	Photographed date
ALPSMF115712740	ALPSMB115712850	2008/3/27
ALPSMF115712735	ALPSMB115712845	2008/3/27
ALPSMF095582740	ALPSMB095582850	2007/11/10
ALPSMF176102735	ALPSMB176102845	2009/5/15

Table 3.7-2   Entry number and photographed date of CORONA images

Forward	Backward	Photographed date
DS1111-1082AF004	DS1111-1082AA010	
DS1111-1082AF005	DS1111-1082AA011	
DS1111-1082AF006	DS1111-1082AA012	
DS1111-1082AF007	DS1111-1082AA013	1970/7/28
DS1111-1082AF008	DS1111-1082AA014	
DS1111-1082AF009	DS1111-1082AA015	
DS1111-1082AF010	DS1111-1082AA016	

3.7.2   Active Fault Traces of the Garni Fault and the Yerevan Fault

Active faults around Yerevan City are shown in Figure 3.7-1. The locations of trench sites (North Garni, Yelpin, and Nor Ughi) carried out for this project are also shown in Figure 3.7-1.

(1) Garni Fault (GF)

The GF is a long active fault with the length of ~200 km and divided into five segments of GF1 to GF5 (Karakhanian et al., 2004; Georisk report). The segments of GF2 from Abovyan to Garni and GF3 from Garni to Yelpin pass through near Yerevan City. These segments are target for scenario earthquakes in this project.

The detailed active fault traces of the GF from Abovyan to Garni (segment GF2) after Georisk report is shown in Figure 3.7-2. The GF is represented as an active fault with clear active fault traces. However, on the satellite photo, it seems that the fault topography is not necessarily distinct. The fault topography such as low fault scarp is clear only on the top of the mountain located at the north of Garni Village (Figure 3.7-3).

The GF crosses a deep gorge with E-W direction on the south of Garni Village, and the fault is exposed on the southern wall (Figure 3.7-4; the location is shown in Figure 3.7-2). The fault is suggested to be the GF. However, fault topography such as a low fault scarp is not recognized on the top of the mountain. It is suspicious whether the fault shown in Figure 3.7-4 is active. The 1679 M 7.0 Garni earthquake has occurred along the segment of GF2. However, it seems that the fault near the surface did not activate during the 1,679 earthquake, since the fault topography is not identified anywhere.

The active fault traces of the GF at Yelpin (segment GF3) are shown in Figure 3.7-5. The fault on the northeastern edge is a major one and small faults of A to D are developed on the west side. As a whole, the fault zone with width of ~1 km is recognized. The sag pond shown in Figure 3.7-6 is reported as typical fault topography by Georisk report. The sag pond is a well-known fault topography that is created by the right-stepping of a right-lateral fault. Three trenches were excavated across these faults. However, an active fault was not confirmed. The pond is not a tectonic product formed by the activity of the GF. Instead an active fault was confirmed along the small fault "D". It is assumed that the GF comprises a 0.5-1 km wide fault zone composed of short intermittent faults rather than a single long fault.

(2) Yerevan Fault (YF)

The YF and its nature are discussed from 1950s (e.g. Aslanyan, 1954, 1958; Gabriyelyan, 1959, 1981). The YF goes through the northeastern margin of Ararat basin and is inferred as an active fault that is tectonically relevant to the formation of Ararat basin. The YF was at first marked as an important active fault close to Yerevan City for seismic hazard assessment of this project. However, the YF was not targeted for active fault mapping at the beginning, since it is thought that the YF is a blind fault.

However, an active fault exposure of Vedi Fault that overlies the Mesozoic bedrocks on the Quaternary deposits was found out near Nor Ughi Village during our preliminary field survey. Furthermore, the pilot trench investigation was carried out near the fault exposure and an active fault was identified in the trench.

The YF is summarized by Georisk report as follows:

Aslanyan(1954, 1958) and Gabriyelyan(1959, 1981) carried out the gravity survey around Yerevan City and found out the NW-SE extending high gravity anomaly on the south of Yerevan City. They suggested active faults on the southwestern and northeastern edges of the high gravity anomaly and called these faults as Parakar north fault and Parakar south fault (red thick solid lines in Figure 3.7-1). These faults represent the central segment of the YF. The mineral springs and travertine are recognized at Dvin and Vedi located on the southeast of Yerevan City. These hot spring processes are inferred to be phenomenon accompanied with the activity of the YF. Aslanyan(1954, 1958) and Gabriyelyan (1959, 1981) inferred the southeastern extension of the YF as shown in Figure 3.7-7. The pilot trench at Nor Ughi Village is located on the fault trace after Gabriyelyan (1959, 1981). Georisk collected and analyzed deep borehole data, and revealed that bedrocks composed of crystalline schist lie at shallow place in depth where the high gravity anomaly is recognized. And the length of the YF is suggested to be 33 km at the maximum based on the structure of Ararat basin (Georisk report). Dvin of ancient capital in Armenia suffered severe damaged from the 863 and 893 earthquakes (Figure 3.7-1). The source of these earthquakes may have been generated by the YF or the GF. According to the mechanism analysis of small to moderate earthquakes around Yerevan City, the reverse fault type is dominant (Tovmasyan, 2008)

The ALOS images at Nor Ughi and Jrashen are shown in Figure 3.7-8 and Figure 3.7-9 respectively. An active fault was identified on the north of Nor Ughi Village of Vedi Fault. However, the main fault is inferred further south, since the terrace is uplifted. At Jrashen the terrace is tilted with inclination of ~10°. This is a kind of deformation of the terrace.
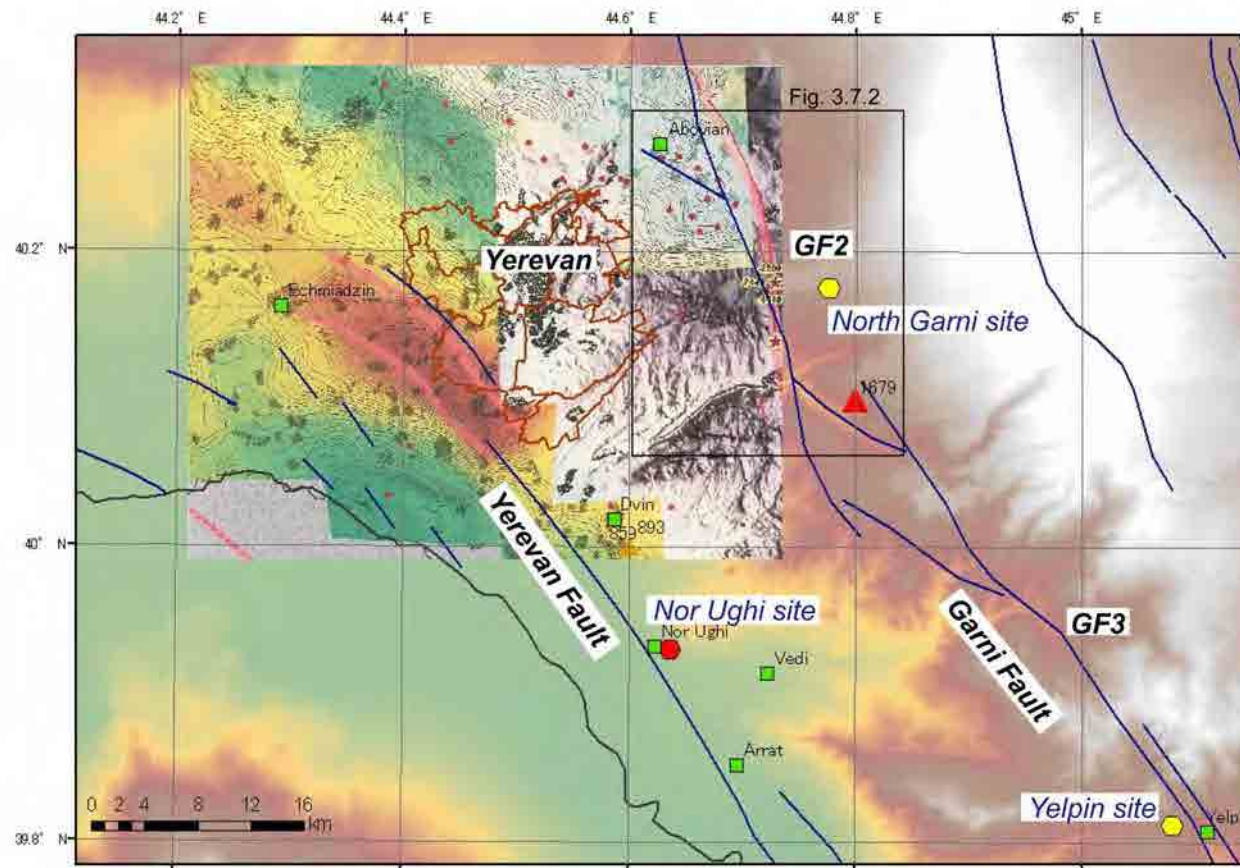
Figure 3.7-1   Active fault map around Yerevan City after Georisk report. The gravity anomaly data are shown in the area including Yerevan City. The segments GF2 and GF3 of the Garni Fault pass through the east of Yerevan City. The Yerevan Fault is inferred on both sides of the northeastern and southwestern edges of high gravity anomaly which is shown in red color.
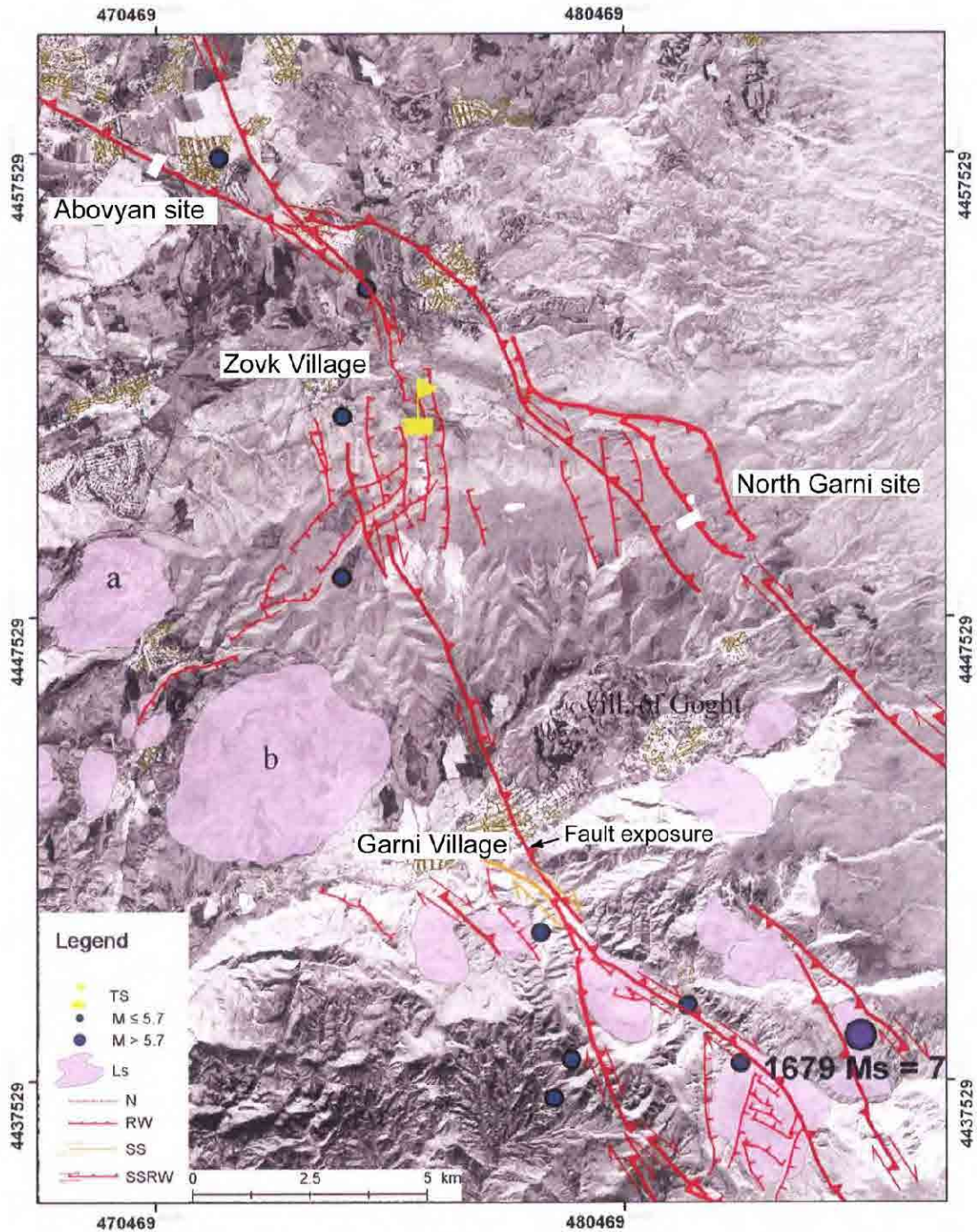
Figure 3.7-2   Detailed active fault traces of GF2 segment of the Garni Fault from Abovyan to Garni Village (Georisk report). The only simplified thick solid lines in Figure 3.7-2 are shown in Figure 3.7-1. The trenches at Abovyan site and North Garni site (white rectangles) were performed for this project, however, an active fault was not confirmed at Abovyan site. The yellow flag is a trench site carried out by Georisk.
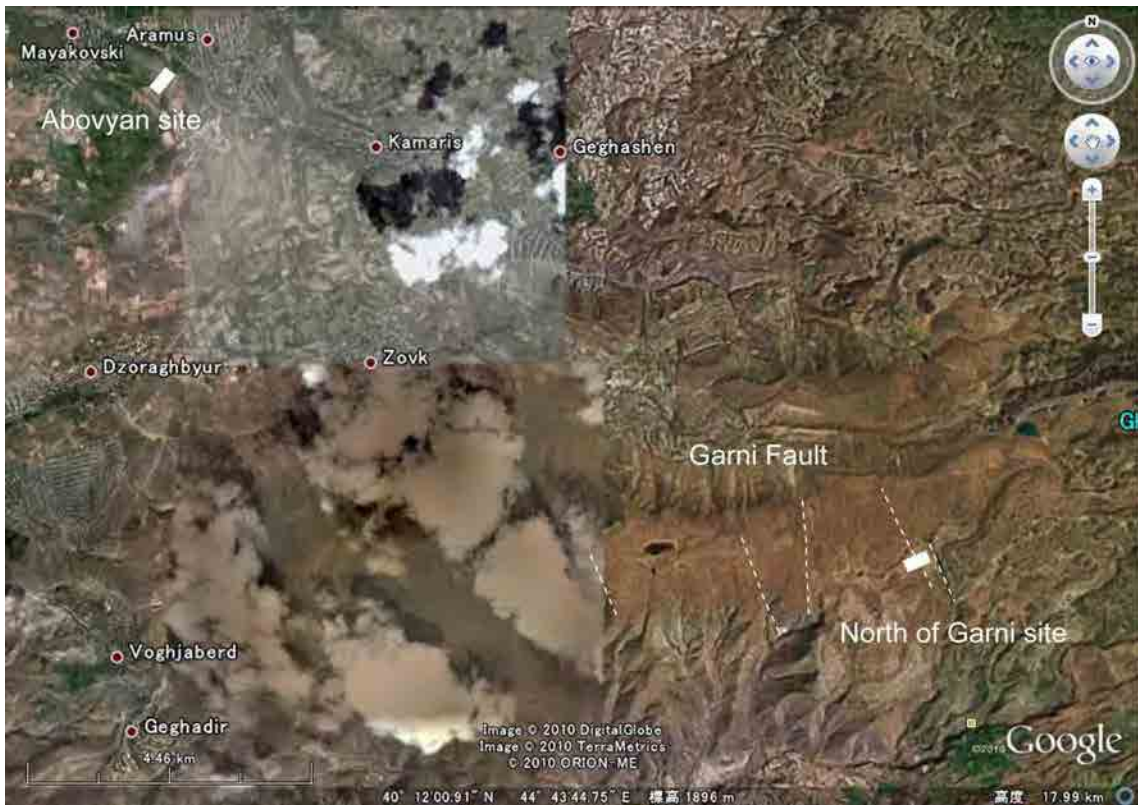
Figure 3.7-3   Active fault traces (white broken lines) on the top of the mountain at the north of Garni Village. At least five N-S trending active faults are inferred.

Figure 3.7-4   Fault exposure of the Garni Fault on the southern wall of the valley, south of Garni Village. The location is shown in Fig. 3.7-2. The fault is clear, however, the fault topography (e.g. a low fault scarp) is not confirmed on the top of the mountain.
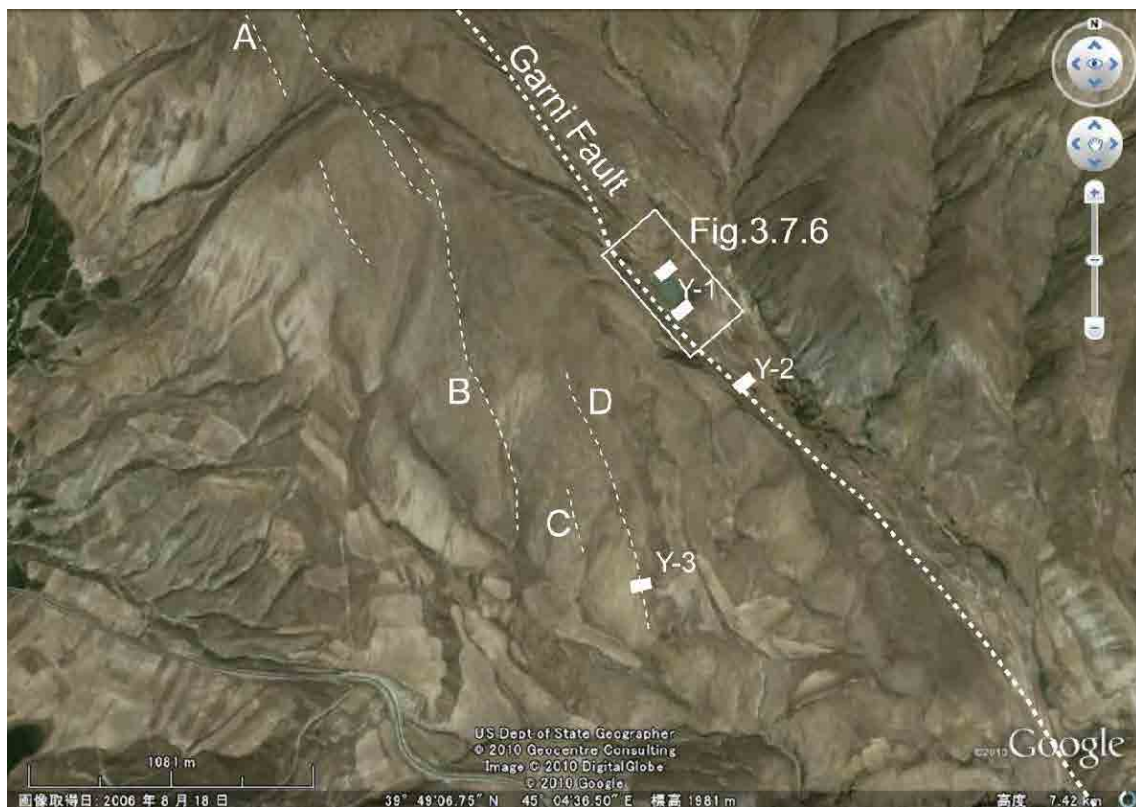
Figure 3.7-5   Active fault traces of the Garni Fault at Yelpin. The thick broken line is a major fault. Three trenches at Y-1 and Y-2 sites were excavated. However, an active fault was not confirmed. Small faults A to D are developed on the west of a major fault. An active fault was identified at Y-3 site.

3-23
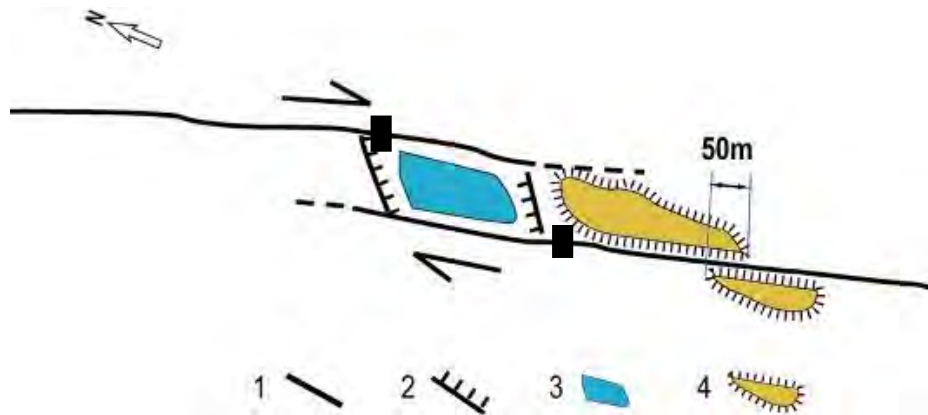
Figure 3.7-6   Active fault traces of the Garni Fault and the location of trench sites (black rectangles). The location is shown in Figure 3.7-5. The figure is after Georisk report. The space with light blue color was suggested to be a sag pond formed by faulting. However, an active fault was not confirmed.
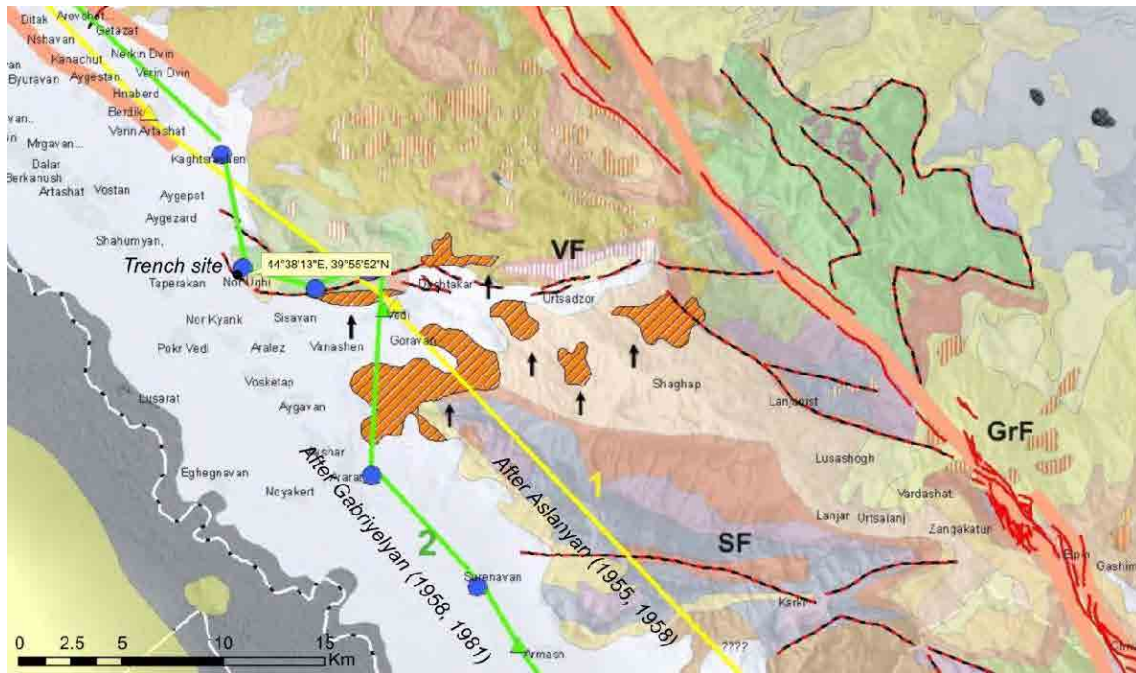
Figure 3.7-7   Active fault traces of the Yerevan Fault around Vedi and Ararat, southeast of Yereban City after Aslanyan (1954, 1958) and Gabriyelyan (1959, 1981). Blue circles and arrows represent the location of mineral springs and travertine respectively. The pilot trench at Nor Ughi is located on the fault trace suggested by Gabriyelyan (1959, 1981). The Vedi Fault (VF) is overlapped on the trench site.
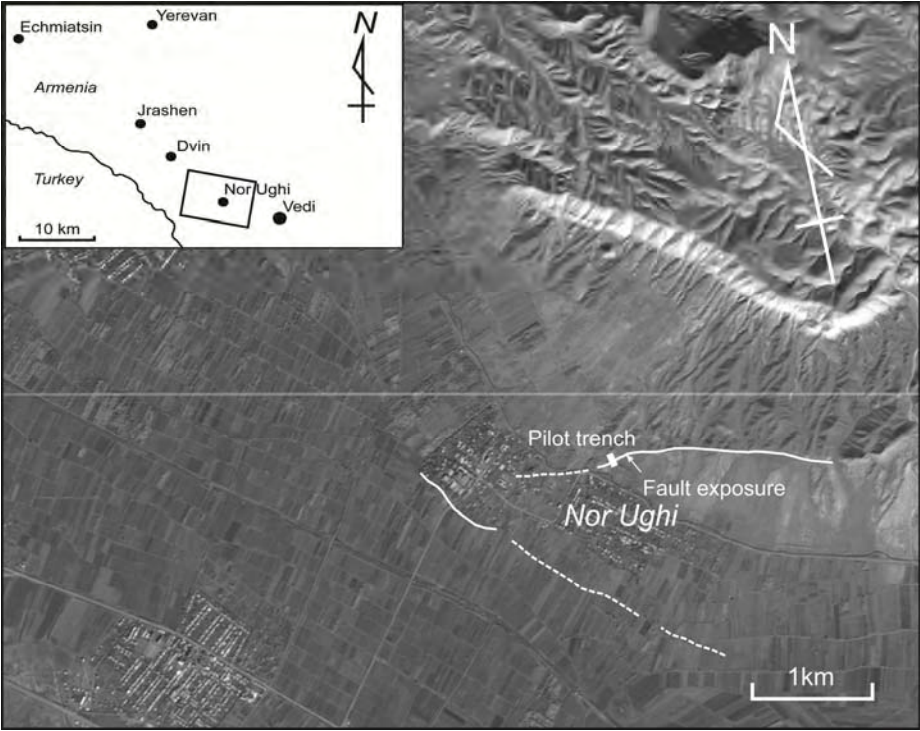
Figure 3.7-8   Inferred fault traces of the Yerevan Fault at Nor Ughi. Background is ALOS image.
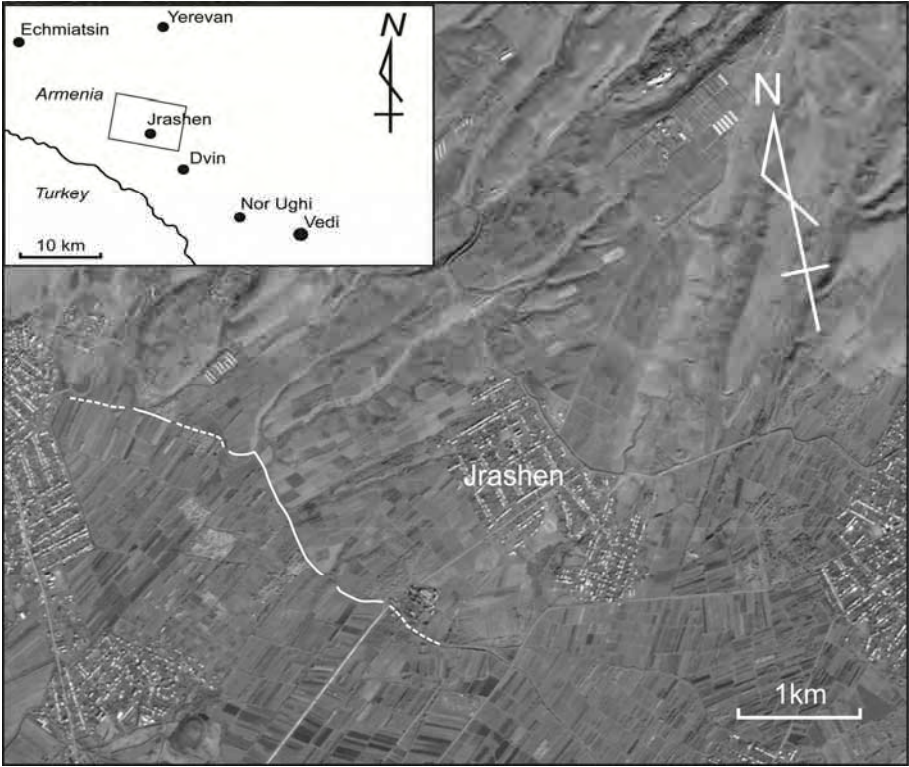
Figure 3.7-9   Inferred fault traces of the Yerevan Fault at Jrashen. Background is ALOS image.

3.7.3   Trench Investigation

(1) Quantity of Trench Investigation

First the trench investigation across the GF was carried out at Y-1 and Y-2 sites of Yelpin (Figure 3.7-5 and Figure 3.7-6). However, an active fault was not confirmed. According to Georisk report, the Garni Fault (GF) at Yelpin is composed of a single major fault and several secondary faults of A to D. However, we reexamined the satellite photo interpretation and reached the view on the GF that there is no major fault and several short faults make a fault zone with width of 0.5-1 km. So the trench site was selected including secondary faults of A to D and an active fault was identified at Y-3 site.

The trench at Abovyan is also located on the inferred major fault of the GF. However, an active fault was not confirmed at this site. Finally an active fault was identified at North Garni site where a secondary fault was inferred. It is significant issue whether there is a major fault along the GF. The modification of active fault map after Georisk report is expected.

First the Yerevan Fault (YF) was thought to be a blind fault. However, the active fault exposure was found out during the preliminary field survey and a pilot trench was excavated at Nor Ughi site across Vedi Fault near Yerevan Fault in order to clarify the nature of the fault.

The quantity of trench investigation is shown in Table 3.7-3.

Table 3.7-3   Quantity of trench investigation

Fault		Location	Quantity	Note
Garni Fault	GF2	Abovyan North Garni	2	GF2 was identified at North Garni
	GF3	Yelpin	4	GF3 was identified at Y-3 site
Vedi Fault near Yerevan Fault		Nor Ughi	1	Pilot trench

(2) Trench Investigation across the Garni Fault (GF)

The Garni Fault (GF) was identified at two sites of Yelpin and North Garni. In this chapter the results of these trenches are reported.

1) Features of deformation and sedimentation of normal fault

The typical deformation and sedimentation of normal fault were observed at the trench sites across the GF. First the features of normal fault are referred.

The deformation of layers accompanied with normal faulting is shown in Figure 3.7-10. Diagram (A) illustrates the deformation of layers on the hanging wall of "listric fault" which decreases the dip angle at deep place. The hanging wall slips along the fault and is separated from the fault scarp, and the layers on the hanging wall sinks down to the open crack. Even if the fault is not a listric one, the surface on the base of fault scarp will be separated by normal faulting, since the fault plane of normal fault is not straight with undulations. Diagram (B) represents the features of fault scarps of normal

fault, i.e. b: bend on the hanging wall, c: formation of fissure-filled deposit. The fissure-filled deposit is called V-shape depression in Japan. Diagram (C) shows the formation process of multiple fissure-filled deposits.

The formation process of "colluvial wedge" is shown in Figure 3.7-11. A: Formation of a fault scarp just after earthquake, B: The fault scarp is collapsed and colluvial wedge is deposited. The colluvial wedge is covered by fine deposits derived from a fault scarp. The colluvial wedge is regarded as a seismic event horizon, since it is formed just after earthquake. The time of paleo-earthquake can be clarified, if the time of colluvial wedge is known.
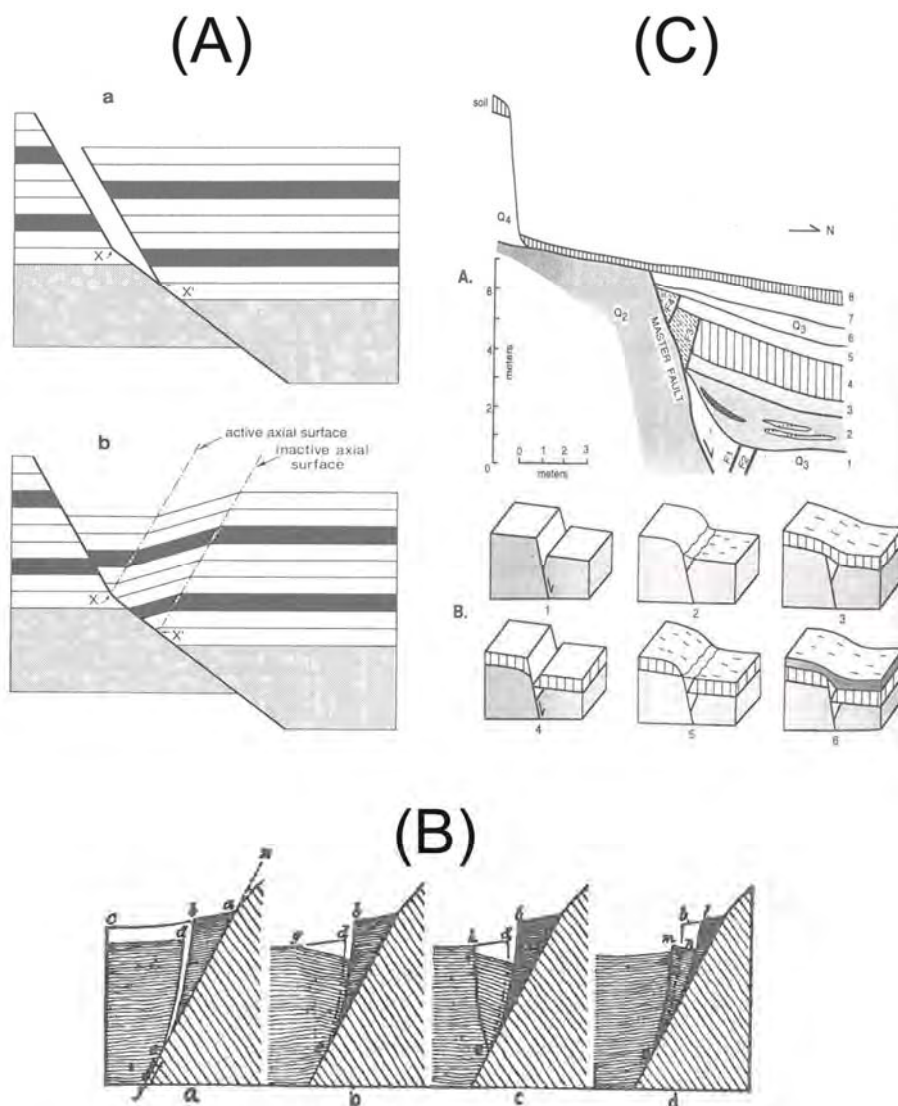
Figure 3.7-10   Deformation of normal fault. A: The hanging wall are separated from the fault scarp and sink down to the open crack due to the decrease of fault dip at deep place (Xiao and Suppe, 1992). B: Diagrams show the deformation of normal fault.(Gilbert, 1890). C: Diagrams shown the creation of two fissure-filled wedges (Wang and Deng, 1988).
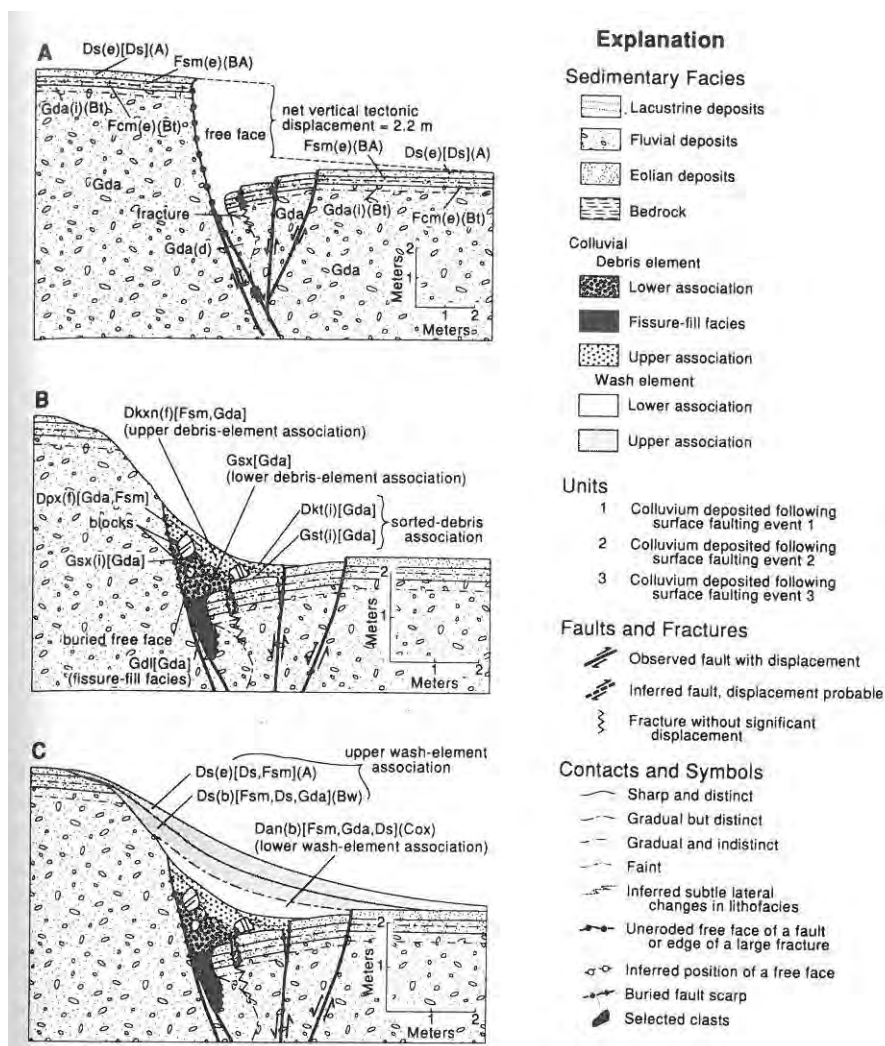
Figure 3.7-11   Process of the formation of "Colluvial wedge" (Nelson, 1992).

2) Trench investigation at North Garni site

i) Geomorphology around trench site

The location of North Garni site is shown in Figure 3.7-2 and Figure 3.7-3. The photographs showing the geomorphology around trench site are shown in Figure 3.7-12 and Figure 3.7-13. The flat land like a terrace is developed on the top of the mountain located at the north of Garni Village. The NNW- SSE trending straight fault scarp with height of 4-5 m was confirmed on the flat surface (Figure 3.7-12). The western side is downthrown and gently inclined to the east (fault scarp side; Figure 3.7-13). The flat surface inclined to the east is a kind of fault topography that is called back-tilting surface, since generally in this region the surface is inclined to the west. The geomorphology such as a straight low fault scarp and back-tilting surface suggested an active fault.

ii) Stratigraphy identified in the trench and its radiocarbon age

A 10 m long, 2 m wide, and 2.0-2.2 m deep trench was excavated across the fault scarp. The log and mosaic photo of south and north walls are shown in Figure 3.7-14 to Figure 3.7-17. The result of ^{14}C dating is shown in Table 3.7-4. All samples were analyzed by AMS (Accelerator Mass

Spectrometry) method. Calendar years were calibrated by the calibration curve with data set of IntCal04 (Reimer et al., 2004). The error range of calendar years is 2σ (95 % probability).

The stratigraphy identified in the trench is divided into units A to F.

Unit A: Grayish-blackish clay with sand and gravel inserting organic soil. The fault scarp was eroded, transported, and then unit A as well as unit B was deposited on the slope. This unit is classified as wash-element in Figure 3.7-11. The fragments of pottery are included in this unit. This unit may be older cultivated soil, since the sedimentary structure is disturbed. ^{14}C dating of four samples of GS-1, GS-2, GN-3, and GN-5 was carried out. However, these samples show older age than unit D. Older charred materials may have been reworked.

Unit B: Whitish sandy silt. This unit as well as unit A is classified as wash-element.

Unit C: Unconsolidated gravel with cobbles. The maximum diameter is ~20cm. This unit is so-called "colluvial wedge" which was derived from the fault scarp just after the earthquake. The colluvial wedge is typical on the south wall. On the north wall, the upper slope of the fault scarp was collapsed, and the boundary between colluvial wedge and landslide is not clear. This unit was first deposited close to the fault scarp and then at far place from the fault scarp. Therefore, the layer close to the fault scarp represents younger age. The samples of GS-4 and GS-5 close to the fault scarp are dated to BC 1420-1260 and BC 1930-1740 respectively.

Unit D: Fissure-filled deposits composed of sand, silt, and crack-filled organic soil. The unit is highly inclined to the east (Figure 3.7-8). The sample of GS-6 on the south wall is dated to BC 1460-1310 that is almost equal to the age of GS-4 of unit C. The crack-filled organic soil is recognized on the north wall (Figure 3.7-16 and Figure 3.7-17). The ages of GN-1 and GN-2 collected from the organic soil are dated to BC 1120-1000 and BC 1380-1260 respectively.

Unit E: Aeolian loam composed of grayish sand with lamina. This unit is weakly consolidated. The sample of GS-3 is dated to BC 5310-5220.

Unit F: Consolidated gravel with cobbles. This unit is thought to be fluvial sediments.

iii) Faults identified in the trench

As shown in log of south and north walls, the main fault comprising a fault scarp is sharply inclined to the west. Several secondary faults are inclined to the east with dip of 50° to 60°. And the V-shape depression is formed by these faults. The main fault inclined to the west is a normal fault in cross section, since the footwall is uplifted and the hanging wall is downthrown.

iv) Time of seismic event

One time seismic event is identified in the trench. Before the seismic event, units D and E covered unit F. By the faulting the east side was uplifted and the fault scarp was created. At the same time, fissures were formed on the base of the fault scarp and unit D was fallen down into the fissures. And the fault scarp was collapsed and the "colluvial wedge" (unit C) was deposited. Continuously the fault scarp was eroded, and units A and B covered unit C.

Judging from this sedimentary process, the seismic event has occurred after the deposition unit D and before the deposition of unit C. The crack on the north wall is filled by organic soils which are older top soil covering the surface just before earthquake. The crack-filled deposits represent the

time just before the seismic event. Considering these, the time of the seismic event is dated to ~BC 1000 (Figure 3.7-19).

v) Displacement

The amount of displacement for a single seismic event is shown in Figure 3.7-20. Because units D and E on the footwall are eroded, the displacement cannot be directly estimated. The amount of displacement is more than 1.4 m. The colluvial wedge is formed by the collapse of the fault scarp. The height of original fault scarp is suggested to be at least twice the thickness of the colluvial wedge (McCalpin edited, 1996). The maximum thickness of the colluvial wedge is 90 cm, so the amount of the displacement is ~1.8 m.
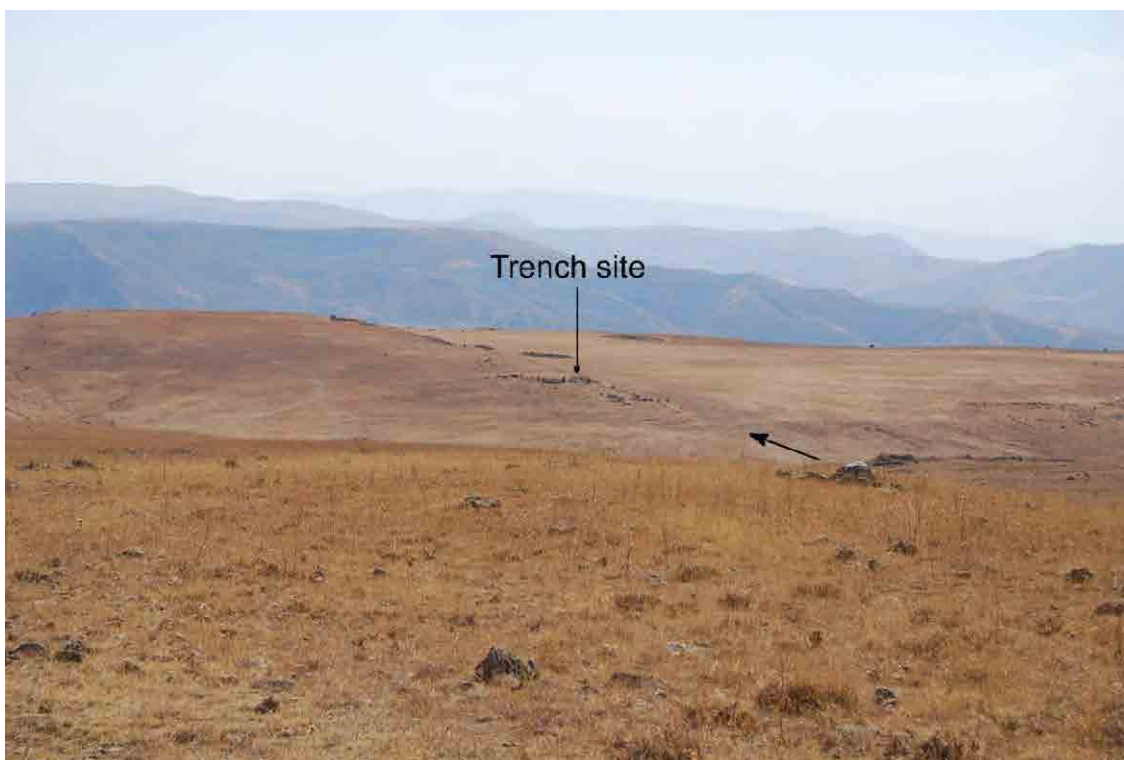
Figure 3.7-12   Geomorphology around North Garni site. The arrow represents an active fault. The fault scarp with height of 4-5 m is clear. View to the south.
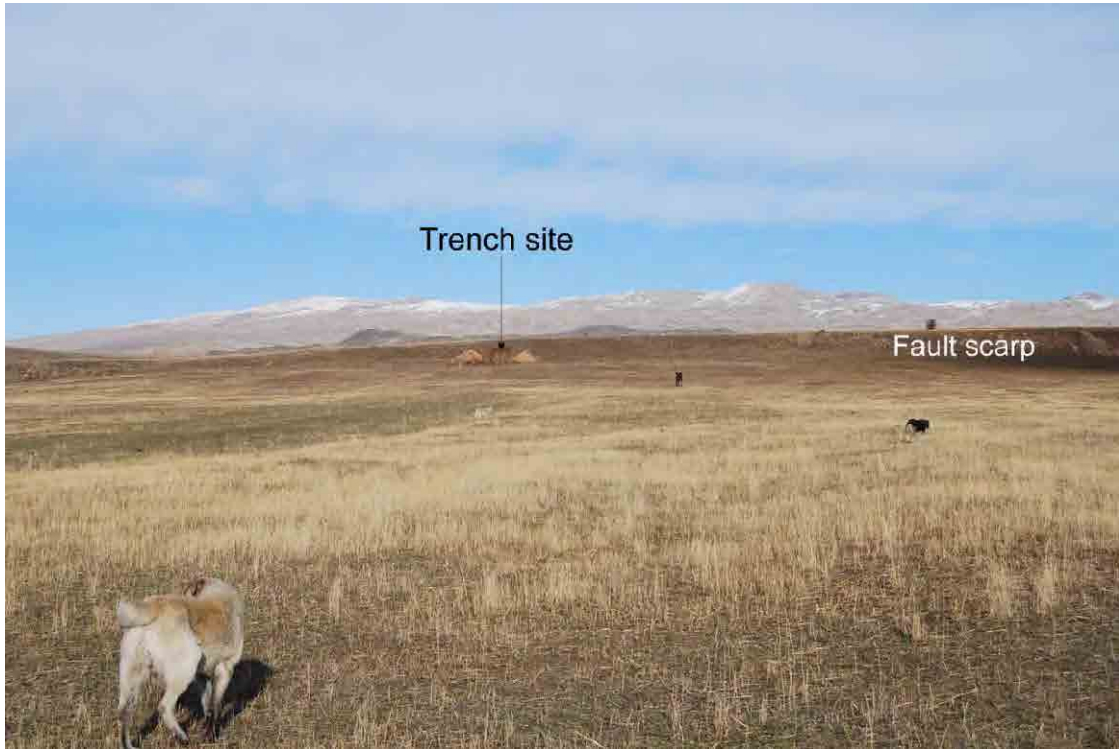
Figure 3.7-13   View of the low fault scarp to the east. The ground surface on the hanging wall (downthrown side) is gently inclined to the east (to the low fault scarp).
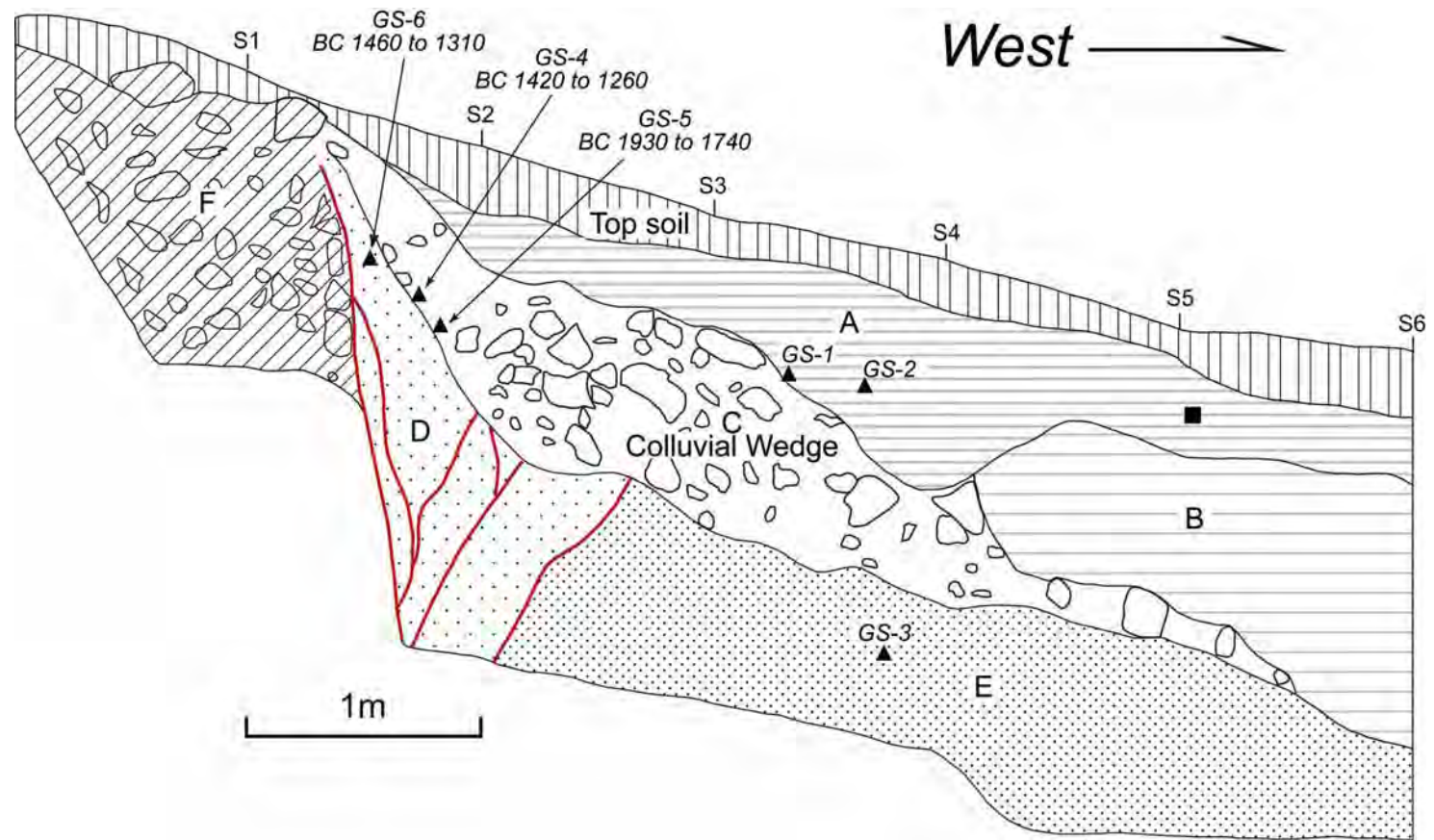
Figure 3.7-14   Log of the south wall at North Garni site. Red solid lines represent active faults. The sedimentary succession in the trench is divided into units A to F. The faults displace units D to F, and are covered by unit C. Unit C is "colluvial wedge" which was deposited by the collapse of the fault scarp just after earthquake. Unit D is a fissure-filled deposits with V-shape. Unit E is weakly consolidated. Triangles and square represent the location of ^{14}C dating and a fragment of pottery respectively.
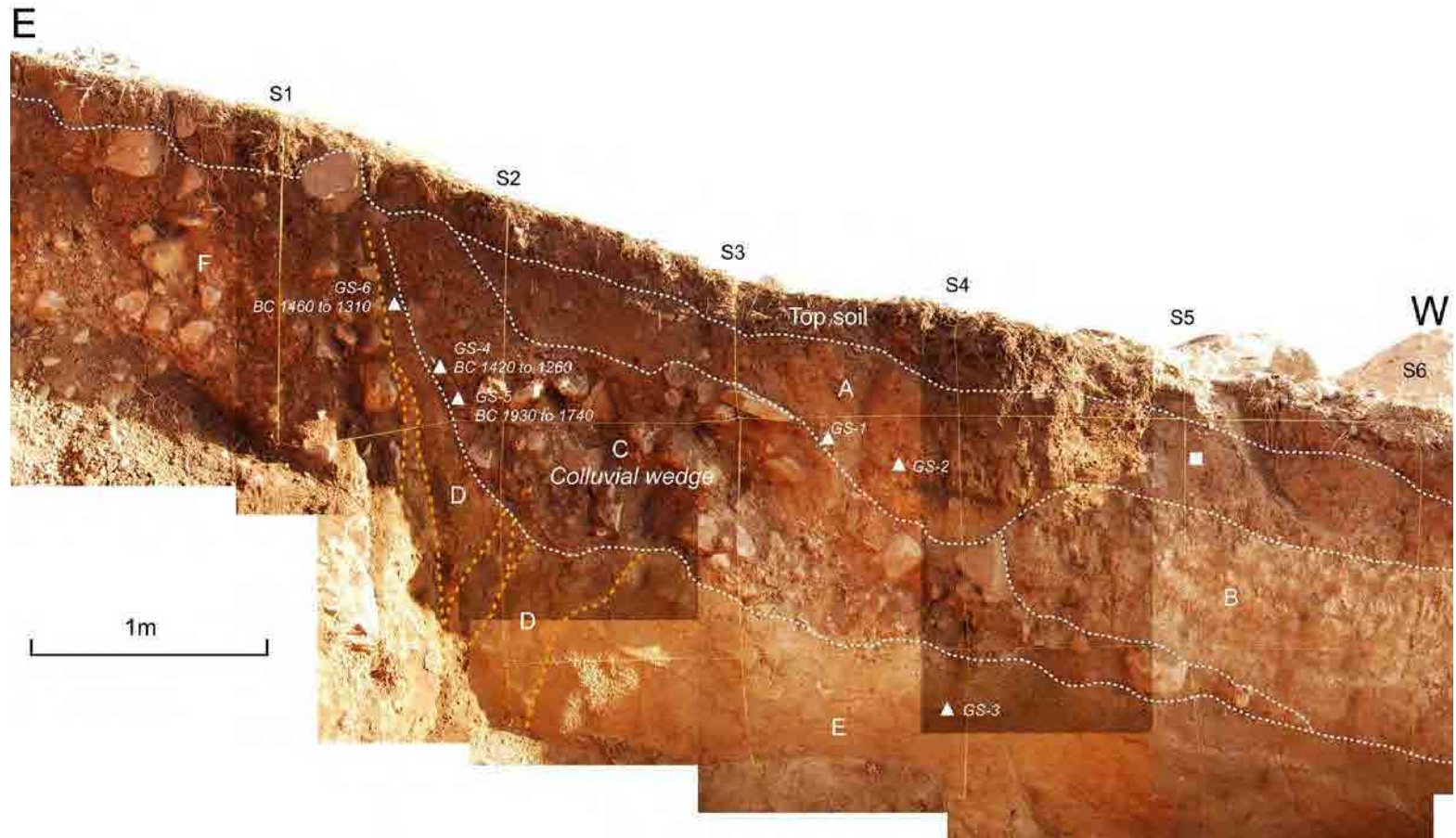
Figure 3.7-15　Mosaic photo of south wall at North Garni site
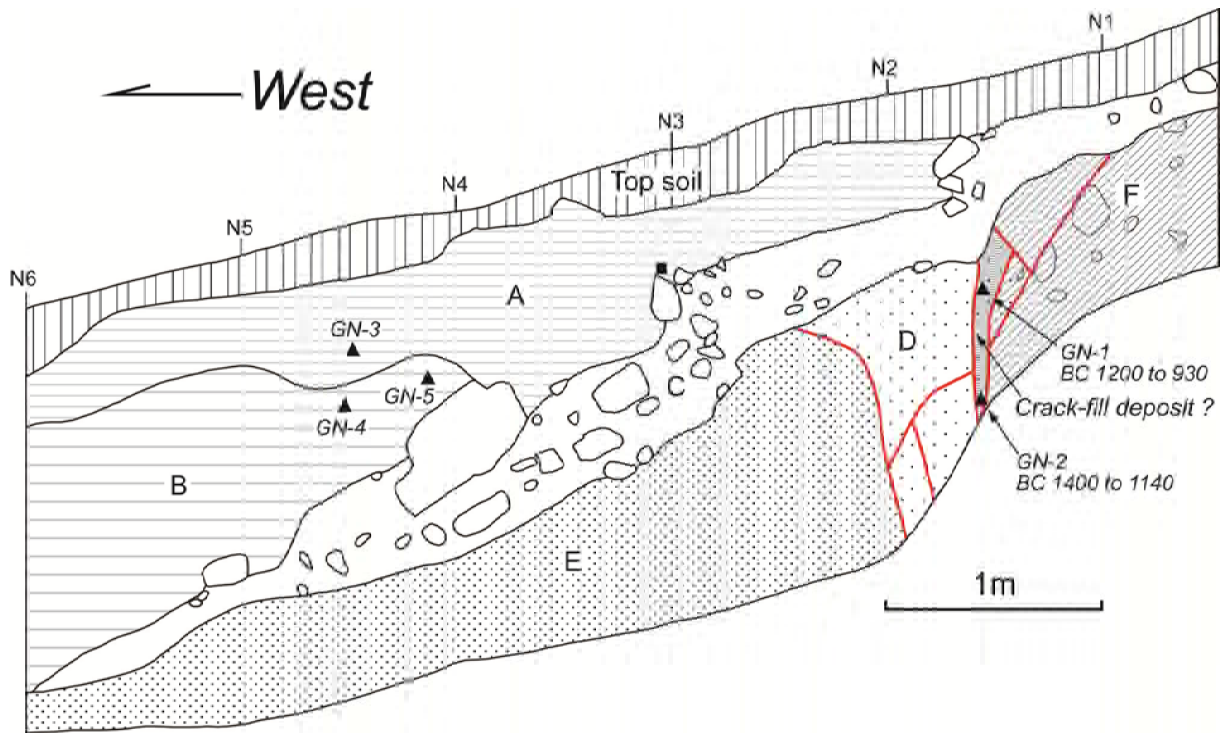
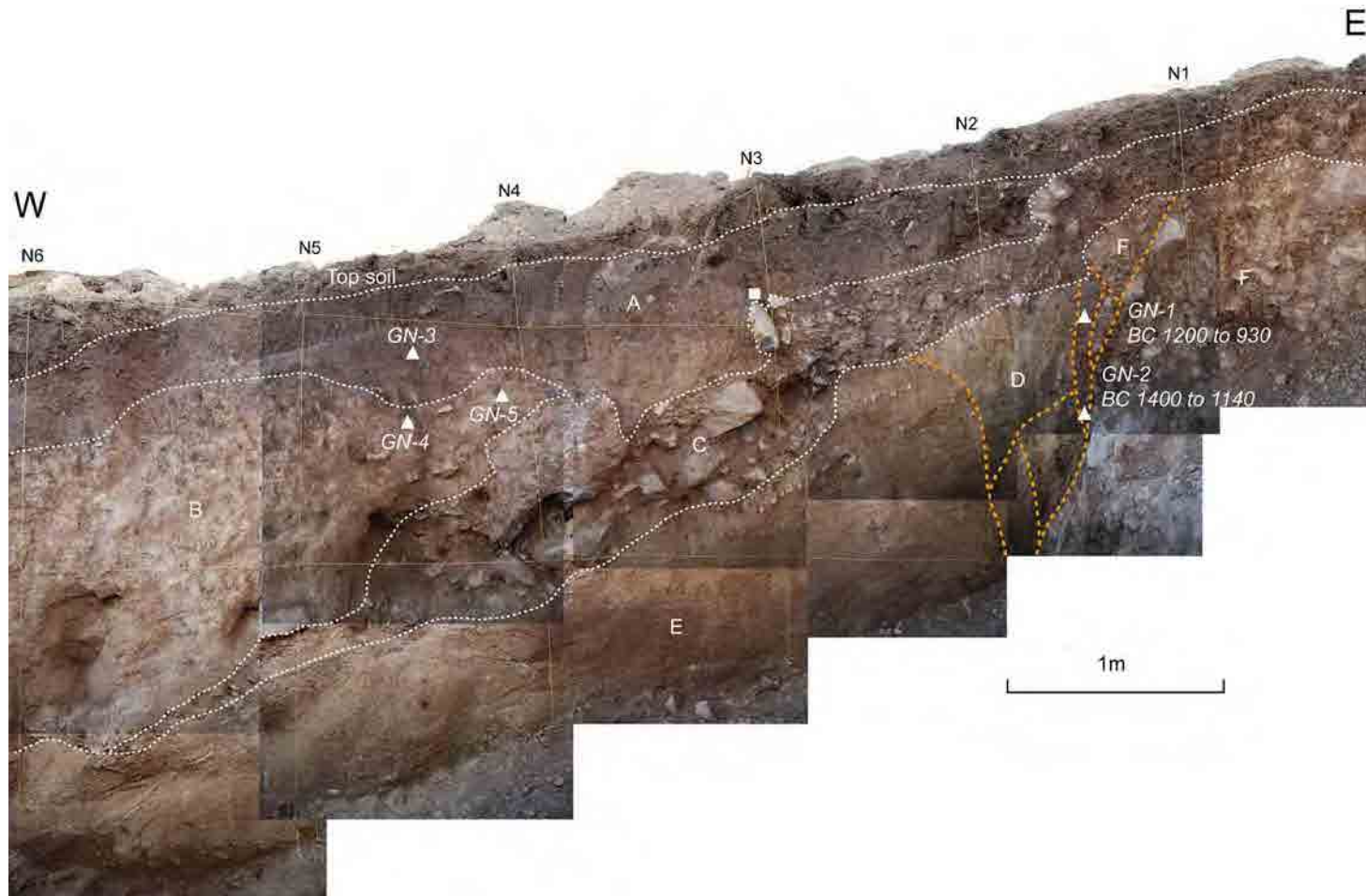Figure 3.7-16   Log of north wall at North Garni site

Figure 3.7-17　Mosaic photo of north wall at North Garni site

Table 3.7-4　Result of ^{14}C dating at the North Garni and Yelpin sites

Trench	Sample number	Laboratory number	Method	Sample	Measured radiocarbon age (yBP)	δ13C (permil)	Conventional radiocarbon age (yBP)	Calender years (2 sigma)
North of Garni	GN-1	Beta-289724	AMS	organic sediment	2870±40	−24.3	2880±40	BC 1200 to 930
	GN-2	Beta-289725	AMS	organic sediment	2990±40	−22.7	3030±40	BC 1400 to 1140
	GN-3	Beta-289726	AMS	organic sediment	4100±40	−24.6	4110±40	BC 2870 to 2500
	GN-4	Beta-289727	AMS	organic sediment	3920±40	−23.6	3940±40	BC 2560 to 2300
	GN-5	Beta-289728	AMS	organic sediment	4390±40	−23.6	4410±40	BC 3320 to 2910
	GS-1	Beta-289729	AMS	organic sediment	4050±40	−23.2	4080±40	BC 2860 to 2490
	GS-2	Beta-289730	AMS	organic sediment	4210±40	−23.0	3030±40	BC 2910 to 2710
	GS-3	Beta-289731	AMS	organic sediment	6230±40	−22.6	6270±40	BC 5320 to 5210
	GS-4	Beta-289732	AMS	organic sediment	3050±40	−23.8	3070±40	BC 1420 to 1260
	GS-5	Beta-289733	AMS	organic sediment	3460±40	−22.5	3500±40	BC 1930 to 1740
	GS-6	Beta-289734	AMS	organic sediment	3090±40	−23.4	3120±40	BC 1460 to 1310
Yelpin	Ye-1	Beta-289735	AMS	organic sediment	2620±40	−23.5	2640±40	BC 840 to 780
	Ye-2	Bete-289736	AMS	organic sediment	1600±40	−24.4	1610±40	AD 380 to 550
	Ye-3	Beta-289737	AMS	organic sediment	2360±40	−24.1	2370±40	BC 530 to 390

Figure 3.7-18   A fissure-filled deposit with V-shape and a colluvial wedge at North Garni site.

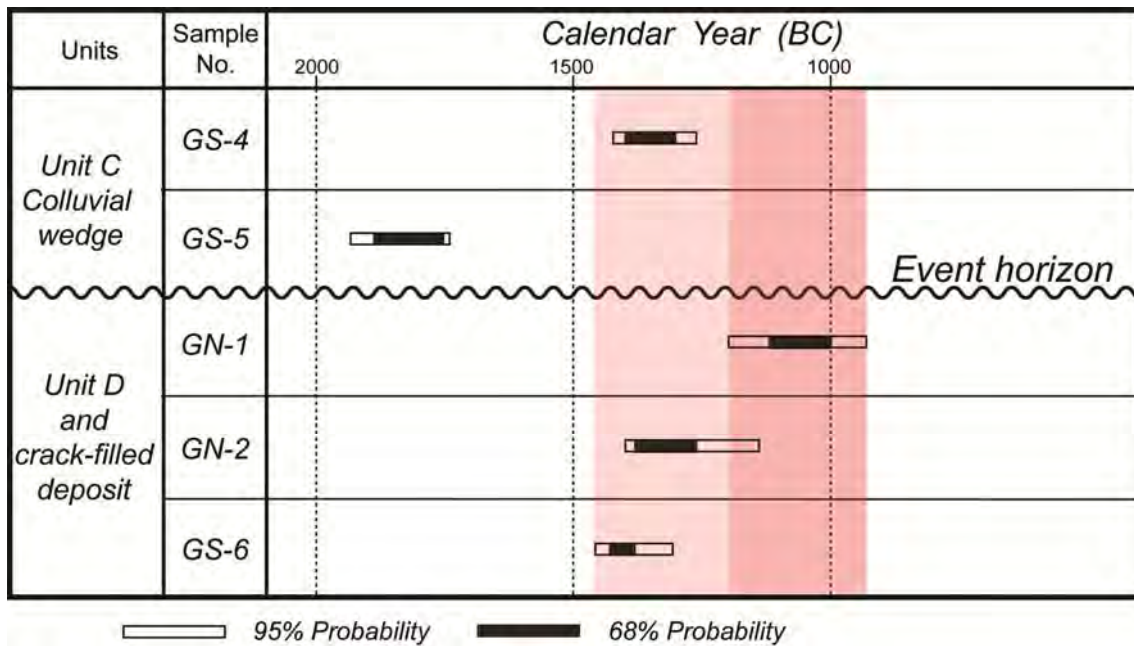95% Probability   68% Probability

Figure 3.7-19   Time of seismic event identified in the trench of North Garni site. The seismic event occurred after the deposition of units D and E, and before the deposition of unit C. The crack on the fault scarp of the north wall was created just after the seismic event, and the existing top soil filled the crack. So the seismic event is inferred to have occurred just after the deposition of a crack-filled deposit.
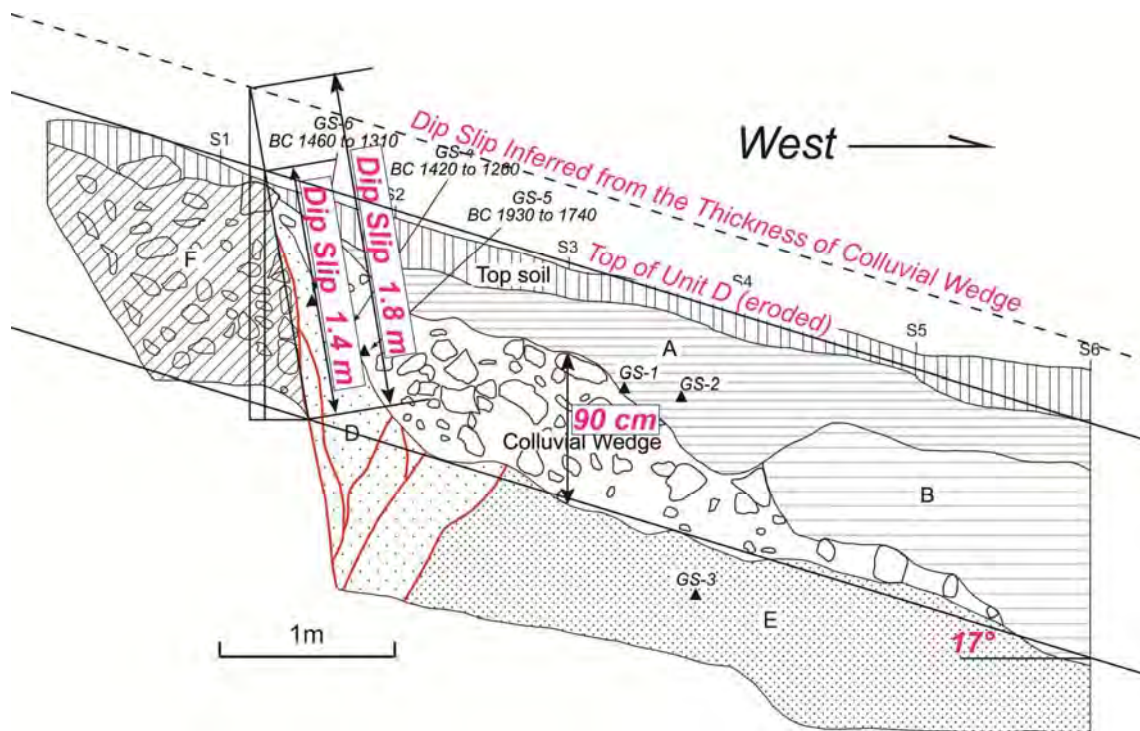
3-37

Figure 3.7-20   The amount of dip slip for a single seismic event inferred on the south wall of North Garni site. The top on the footwall is eroded. The displacement for a single seismic event is over 1.4 m. The colluvial wedge is formed by the collapse of the fault scarp. The height of the fault scarp is at least two times of the thickness of the colluvial wedge. The maximum thickness of the colluvial wedge is 90 cm, so the displacement is inferred to be ~1.8 m.

3) Trench investigation at Yelpin site

 i) Geomorphology around trench site

The location of Yelpin Y-3 site is shown in Figure 3.7-5. The photographs of the geomorphology around Y-3 site are shown in Figure 3.7-21 to Figure 3.7-23. The NNW-SSE trending low fault scarp is observed on the mountain with poor vegetation. The low fault scarp is clear and can be found even on Google Earth Image. The straight low fault scarp with height of ~1 m is recognized at Yelpin Y-3 site. The fault exposure was found out on the road cutting which was built for the construction of pipeline of natural gas. As shown in Figure 3.7-24, The western and eastern sides of the fault are composed of the Paleogene Limestone and the Quaternary deposits respectively. The Quaternary deposits are weakly consolidated by the cementation due to dry. Fissure-filled deposits (V-shape depression) are recognized on the top of the cutting wall. Unconsolidated gravels are sunk to the fissure (Figure 3.7-25). The vertical slickenside is recognized on the fault plane of the Paleogene Limestone (Figure 3.7-26).

 ii) Stratigraphy identified in the trench and its radiocarbon age

A 10 m long, 2 m wide, and 2.0-2.5 m deep trench was excavated near the fault exposure. The log and mosaic photo of south wall is shown in Figure 3.7-27 and Figure 3.7-28 respectively.

The stratigraphy identified in the trench is divided into units A to D. Two V-shape depression, V1 and V2, are observed in the trench (Figure 3.7-29). The result of ^{14}C dating is shown in Table 3.7-4.

Unit A: A debris flow deposit composed of gravel with angular to sub-angular pebbles-cobbles. This unit is poorly sorted parallel to the surface. ^{14}C dating of the samples of Ye-2 is carried out. It is dated to AD 380-550.

Units B and C: Reddish brown sandy clay with gravel. These units with distinct bedding parallel to the surface are weakly consolidated by cementation due to dry. Unit B includes gravels, while there is less gravel in unit C. These units may be aeolian loams inserting debris flows.

Unit D: Paleogene Limestone. The fault gouge with thickness of 40 cm is recognized.

V1: Fissure-filled deposits V1 is composed of gravel with cobbles. The weak bedding is recognized and represents the dip of 40° to 50° inclined to the west (fault scarp side). The sedimentary features of V1 are similar to unit A, however, the gravels are bigger than those of unit A. V1 may include the gravels which were fallen from the fault scarp. It is not known whether the boundary between unit A and V1 represents a fault or merely exhibits a bend.

V2: V2 is composed of gravel including clasts of sandy silt (unit C) and limestone. The clasts of unit C are rotated. The boundary between V2 and units B-C is separated and clay supplied from the surface is filled. The crack is also filled by clay at horizontal marker S3 and covered by unit A.

 iii) Time of seismic event

Twice seismic events are identified in the trench by the fissure-filled deposits of V1 and V2. The latest event that created V1 has occurred after the deposition of unit A. The time of the latest event is dated to after AD 380-550. The penultimate event that created V2 has occurred after the

deposition of unit B and before the deposition of unit A. However, the radiocarbon age of units B and C is not obtained, so the time of the penultimate event is unknown.

v) Displacement

The height of fault scarp shown in the right top of Figure 3.7-27 is 50 cm to 1m. This represents the amount of displacement for a single seismic event.
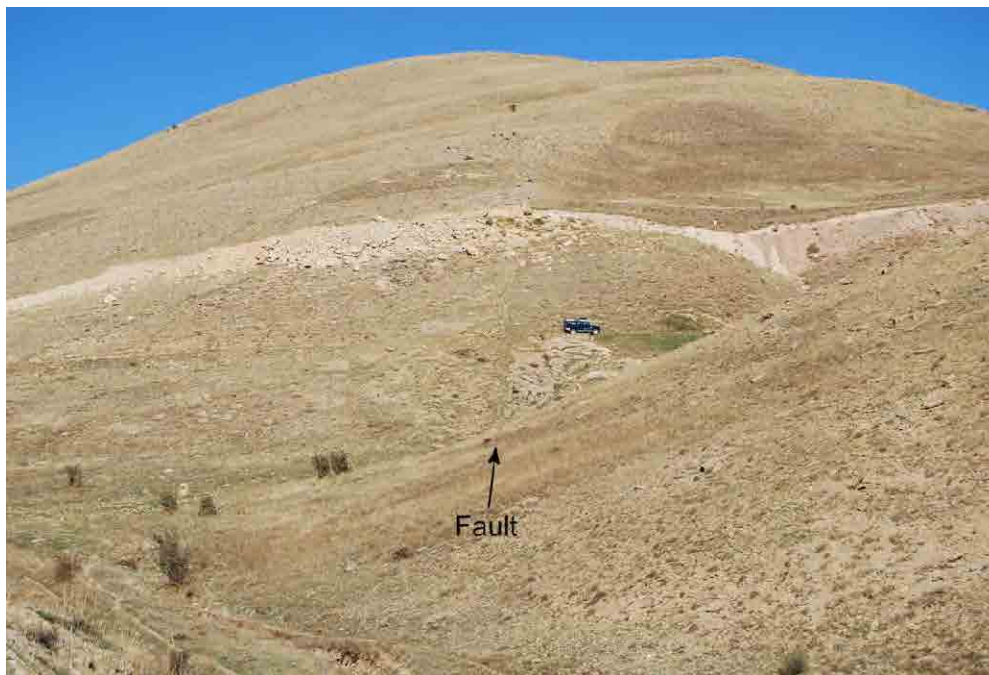

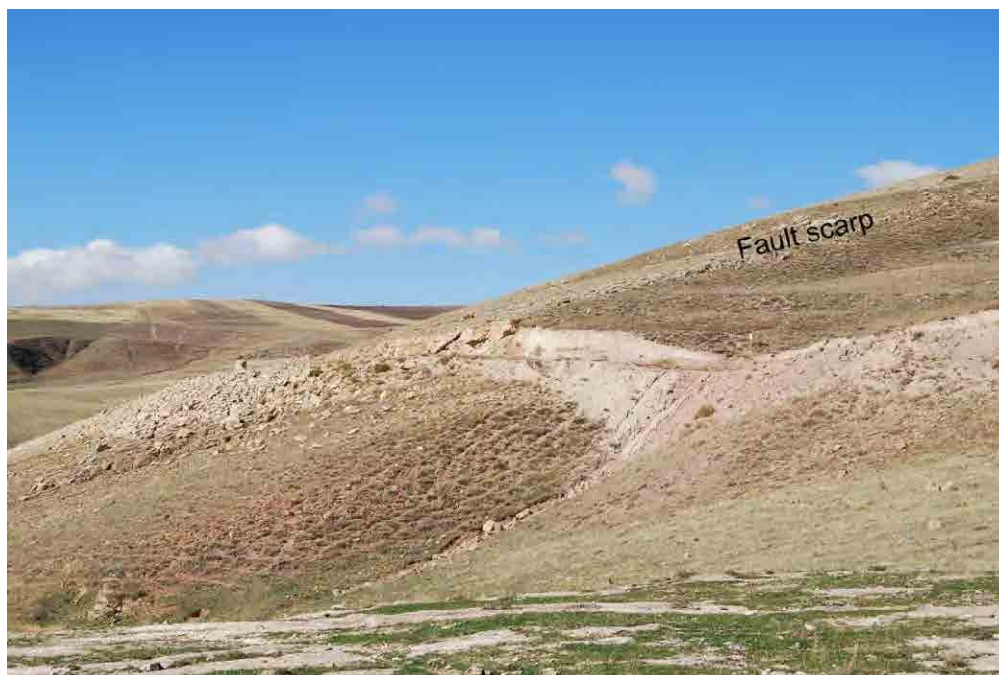Figure 3.7-21   Active fault trace at Yelpin. View to the north.

Figure 3.7-22   Low fault scarp at Yelpin. The fault exposure was found out on the road cutting. View to the west.

Figure 3.7-23   Two trenches were excavated across the low fault scarp.

Figure 3.7-24　Photograph of fault exposure. The left side and right side are composed of the
Paleogene Limestone and the Quaternary deposits respectively.

Figure 3.7-25   Fissure-filled deposits with V-shape on the top of road cutting. The deposits are composed of unconsolidated gravel with cobbles.

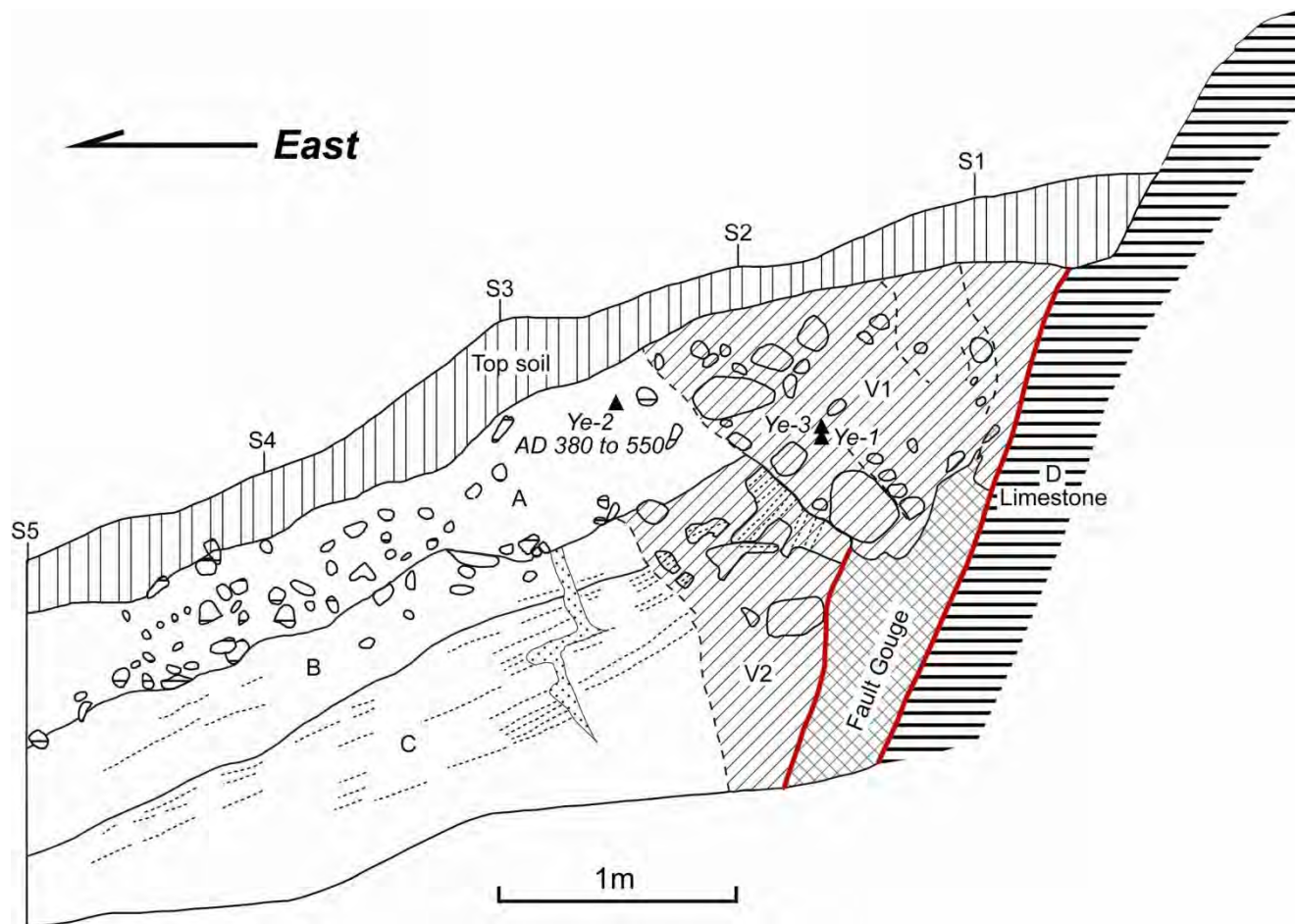Figure 3.7-26   Vertical slickenside is recognized on the fault plane. This indicates a normal fault.

Figure 3.7-27   Log of south wall at Yelpin Y-3 site. Red lines represent active faults. Two V-shape depressions, V1 and V2, are recognized in the trench. Triangles represent the location of ^{14}C dating.
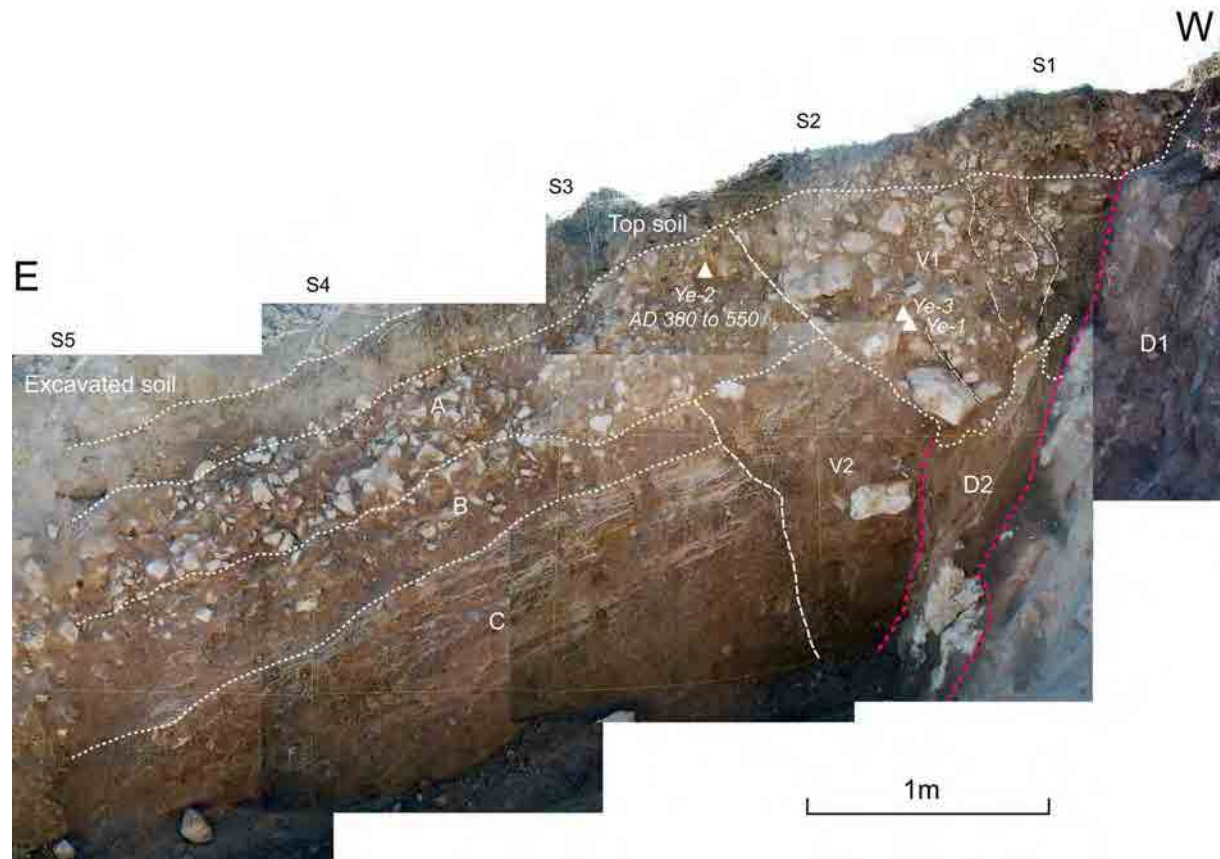
Figure 3.7-28   Mosaic photo of south wall at Yelpin Y-3 site. D1: Limestone, D2: fault gouge of Limestone.

Figure 3.7-29   V-shape depressions at Yelpin Y-3 site.

(3) Pilot Trench Investigation at Nor Ughi Site

The location of the pilot trench at Nor Ughi site across Vedi Fault is shown in Figure 3.7-7 and Figure **3.7-8**. Nor Ughi Village is situated near the northeastern margin of Ararat basin, 30 km southeast from Yerevan City. The Google Earth image around Nor Ughi Village is shown in Figure 3.7-30. The straight low scarp was found on the north of Nor Ughi Village. The geomorphology in this region is severely modified by agriculture. However, the low scarp that makes the topographic boundary between the hill and uplifted surface is clear. The low scarp was indicative of a fault scarp. So we carried out the field survey along the low scarp and found out the fault exposure (Figure 3.7-31 and Figure **3.7-32**).

The fault, which overlies the Mesozoic sediments on the unconsolidated Quaternary deposits, is a reverse one with strike and dip of N62°W, 17°NE. The slickenside on the fault plane shows the direction of N20°E (Figure 3.7-32). The pilot trench was excavated across the fault at the west of the fault exposure, since the fault exposure is parallel to the fault strike and the observation is difficult.

The mosaic photo is shown in Figure 3.7-33. The sedimentary succession identified in the trench is divided into Gravel 1, Gravel 2, Sand, and Cretaceous sedimentary rocks.

Gravel 1 and 2: Fluvial deposits composed of gravel with angular to sub-angular pebbles. These layers are suggested to be deposited by small channels. The lamina representing the flow from east to west is observed on the fault scarp.

Sand: Weakly consolidated grayish medium to coarse sand. This layer may be aeolian loam.

Cretaceous sediments: Grayish-greenish color sandstone. The fault gouge with thickness of ~50 cm is recognized. There are many calcareous veins of travertine in the sedimentary rocks. However, the calcareous veins are broken by the faulting in and near the fault gouge.

Two fault strands F1 and F2 overlying the Cretaceous sediments on the unconsolidated Quaternary deposits are identified in the trench. F1 strand dips with 26°. Judging from the stratigraphic cross-cutting relationship, twice seismic events are identified in the trench. F2 fault strand displaces Sand layer and is covered by Gravel 2 layer. The penultimate seismic event has occurred after the deposition of Sand layer and before the deposition of Gravel 2 layer. F1 fault strand displaces all layers. The latest event has occurred after the deposition of Gravel 1 layer. However, the time of seismic events are unknown, since dating samples for radiocarbon dating were not collected.

(Dr. A. S. Karakhanian of IGS insisted that the older tephra during the Middle to Early Quaternary time? is recognized in the Gravel 1 and 2 layers, therefore, the faults identified in the trench are old and not active, since the Gravel 1 and 2 layers are inferred to be older deposits. However, the tephra could not be found in Gravel 1 and 2 layers. Even if there is tephra in the Gravel 1 and 2 layers, the tephra is not original one. It is secondary deposit, since the Gravel 1 and 2 are small channel deposits under fluvial environment. This simply means that the Gravel 1 and 2 are younger than the age of the original tephra. Considering the unconsolidated nature of the Gravel 1 and 2, these layers are young deposits, maybe Holocene to Late Pleistocene time).

The amount of net-slip cannot be exactly estimated, since the top of hanging wall is eroded. It is more than 2.7 m (Figure 3.7-34).

The fault identified at Nor Ughi site corresponds with the western extension of the Vedi Fault. The Vedi Fault is a geological fault, not active. The western part of the Vedi Fault may have a possibility to be activated accompanied with the rupture of the Yerevan Fault which should be inferred more south on the topographic boundary between the uplifted surface and the Alluvial Plain. The fault identified in the trench may be a secondary one. However, in order to verify this issue, it is inevitable to detect the rupture evidence of the Yerevan Fault.
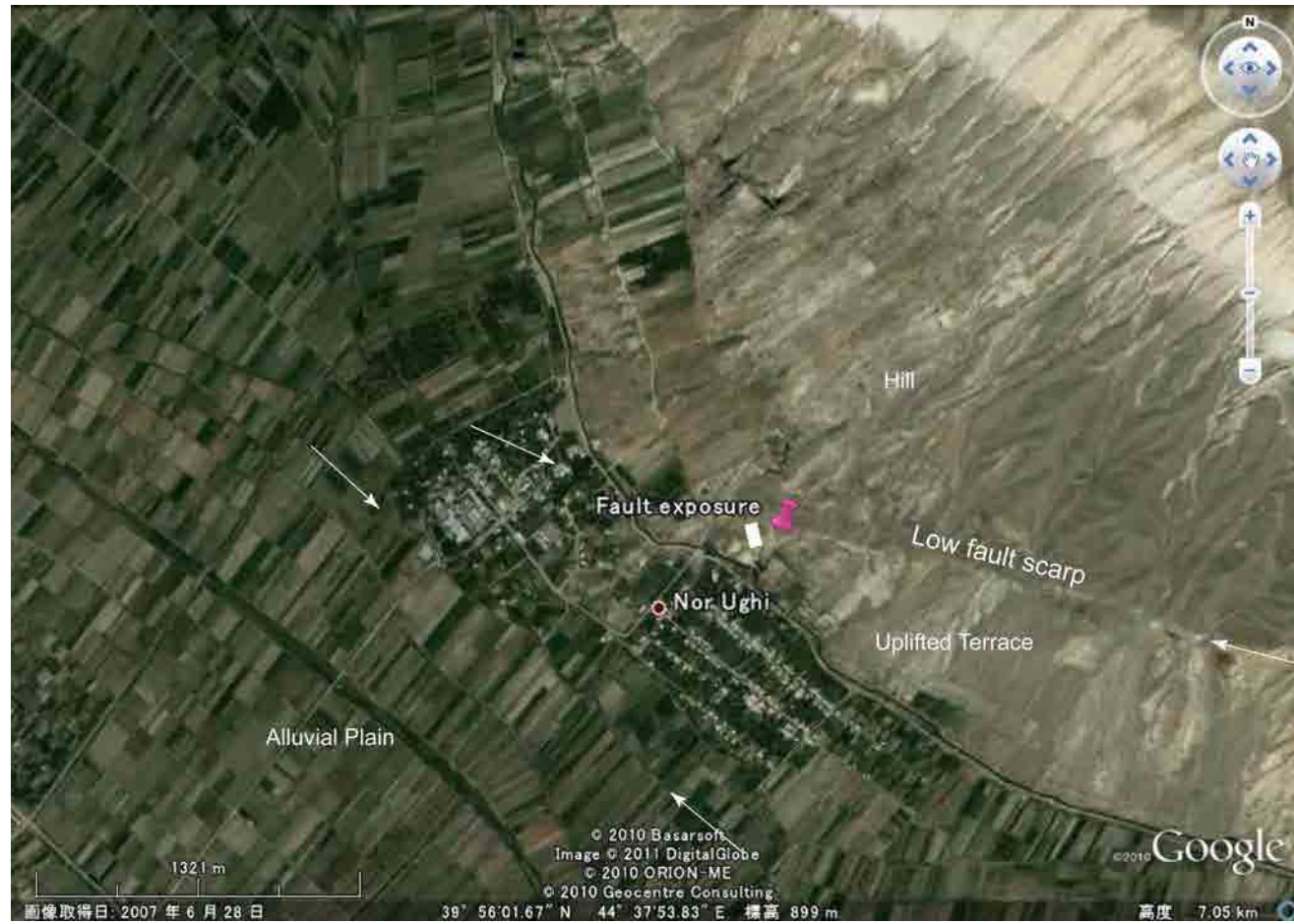
Figure 3.7-30   Fault exposure (pink pin) on the north of Nor Ughi Village and the location of a pilot trench (white rectangle). A straight low fault scarp is clear on the topographic boundary between the Hill and uplifted terrace. However, a major fault is inferred on the topographic boundary between the uplifted terrace and the Alluvial Plain, since the terrace around Nor Ughi Village is uplifted.

Figure 3.7-31   Fault exposure at the north of Nor Ughi Village where a person is standing. The fault overlies the Mesozoic sediments on the Quaternary deposits. The pilot trench was excavated at the left side of the exposure.

Figure 3.7-32   Photograph of the fault. The upper part and lower part are the Mesozoic sediments and the Quaternary deposits respectively. The Quaternary deposits are composed of unconsolidated gravel. The strike and dip of the fault is N62°W, 17°NE and the direction of slickenside is N20°E.
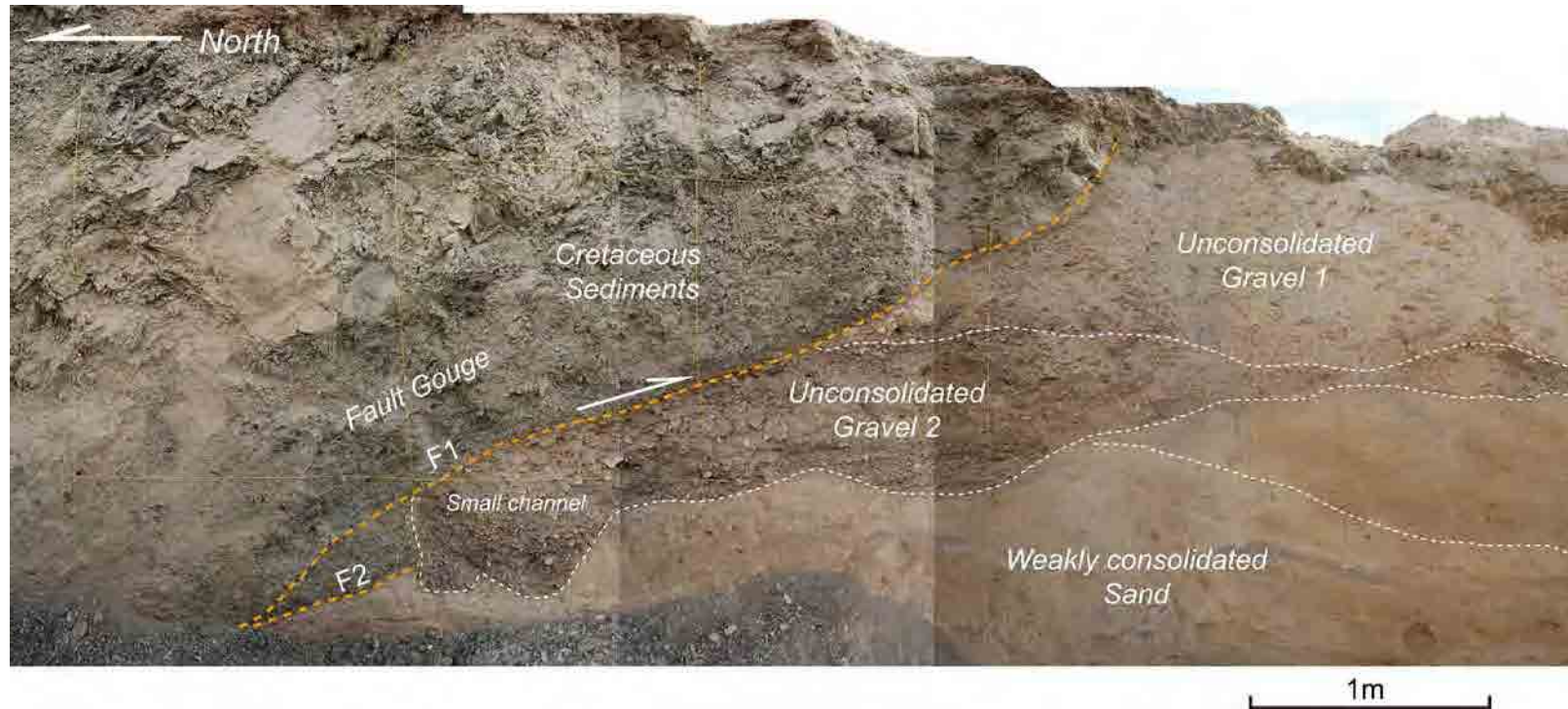
Figure 3.7-33   Mosaic photo of east wall at the pilot trench site of Nor Ughi. The Mesozoic sediments are overlain on the Quaternary deposits by a low-angle reverse fault. The Quaternary deposits are divided into weakly consolidated Sand, unconsolidated Gravel 2, and Gravel 1. Two fault strands F1 and F2 are recognized and twice seismic events are inferred. F2 fault strand displaces Sand and is covered Gravel 2. F1 fault strand displaces all layers.
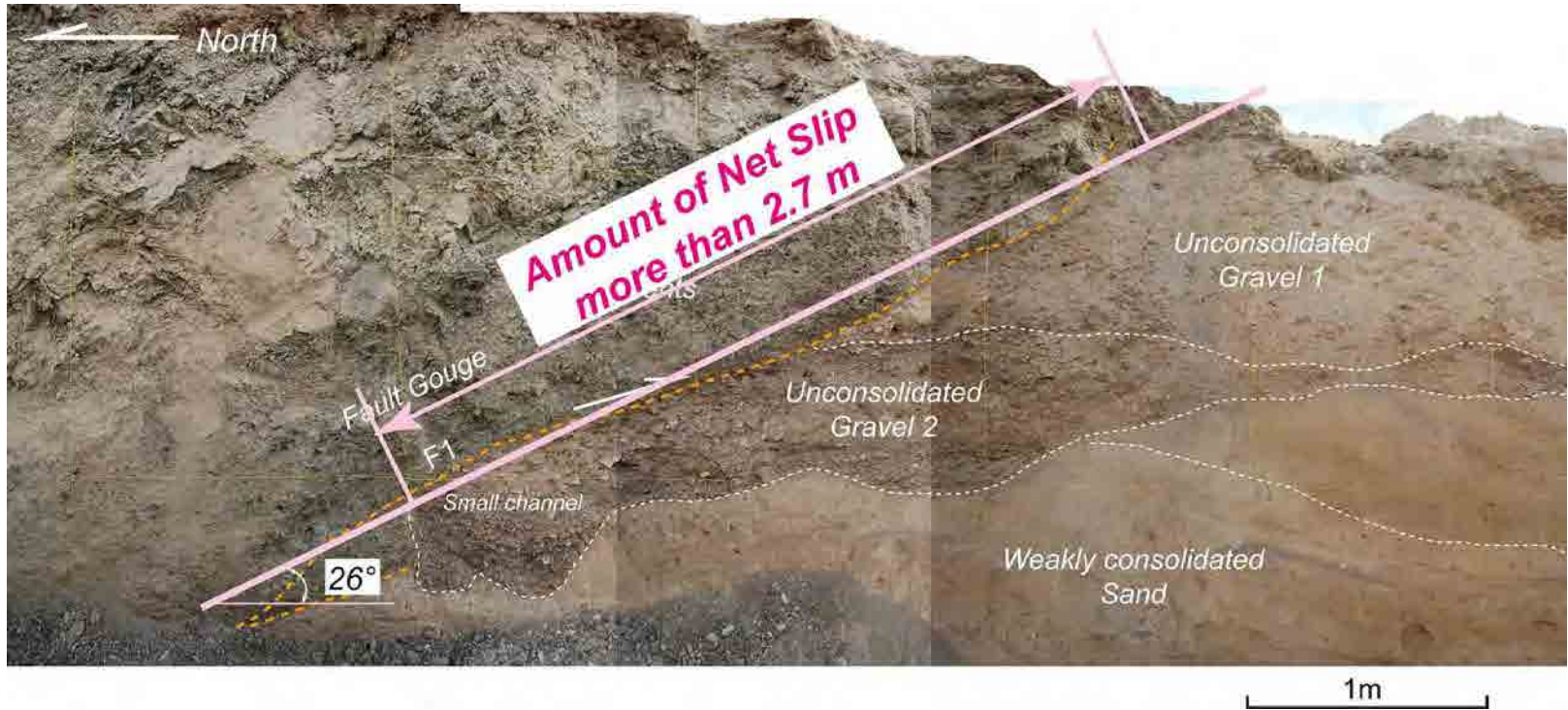
Figure 3.7-34   Amount of net slip along F1 fault. The top on the hanging wall is eroded. The amount of the net-slip is more than 2.7 m.

3.7.4 Probability of Future Earthquake Occurrence

The 50 years probability of future earthquake occurrence based on the BPT model (Brownian Passage Time Model) is shown in Table 3.7-5. The Ms 6.9 Spitak earthquake has occurred in 1988 along the GF1 segment. According to the trench investigation across the GF1 segment carried out after the earthquake, the recurrence period is suggested to be 4000 to 5000 years (Philip et al., 1992). The 1679 M 7.0 Garni earthquake has occurred along the GF2 segment. And the paleo-earthquake during ~BC 1000 is inferred by the trench investigation at North Garni site across the GF2 segment. The recurrence period is suggested to be ~2700 years. The recurrence period of GF3 segment is not clarified, however, the GF3 segment has ruptured after AD 380 to 550. The 50 years probability of future earthquake occurrence along the GF1, GF2, and GF3 segments is small, since the recurrence period of these segments is ~2700 years and these segments has ruptured during historic age or recent time.

Concerning the Yerevan Fault, it is not known whether the Yerevan Fault has ruptured during historic age, and the recurrence period is also unknown. There are historic documents that Dvin of the ancient capital in Armenia has suffered severe damages in AD 893. This earthquake may have been generated by the Yerevan Fault, since Dvin is situated close to the Yerevan Fault. However, there are no evidences that the Yerevan Fault has ruptured in AD 893. The trench investigation across the Yerevan Fault is expected. And next 3.7.5 describes the results of additional trench survey for Yerevan Fault in 2011.

Table 3.7-5   50 years probability of future earthquake occurrence on the active faults around Yerevan City

Segment	Events	Reccurrence Period (year)	Elapsed Time since Latest Event (year)	50 Years Prob. (%)	Estimated Magnitude (Mw)
Garni Fault					
GF1	1988 Spitak earthquake (Ms 6.9)	4000-5000[3] ?	23	0.0	6.9
GF2	1679 Garni earthquake (M 7.0) [1] BC 1000[2]	2700[2]	332	0.0	6.8-7.0[2]
GF3	after AD 380 to 550[2] (AD 893 ?)	2700[2] ?	1118	1.2	6.8-7.0[2]
GF4	?	?	?	?	?
GF5	AD 910 ?	?	?	?	?
Yerevan Fault					
Central Segment	AD 893 ?	?	?	?	6.7-6.9[2]

1) Georisk report, 2) This study, 3) Philip et al. (1992)

3.7.5 Additional Trench Survey across Yerevan Fault

As per the initial plan for the project, the trench survey at Yerevan Fault (see Figure 3.7-35) was judged difficult, because the fault would be a blind fault. For that reason, the trench survey, targeted mainly Garni Fault, was conducted at the two sites and then the fault evidences were found. However, at 2010

end, during the supplementary survey for Yerevan Fault on site, an outcrop of fault was found at Nor Ughi site (Figure 3.7-30). The pilot trench at Nor Ughi 1-1 point, west of the fault outcrop, confirmed a clear reverse fault (Figure 3.7-33 and Figure 3.7-34).

The fault found at Nor Ughi 1-1 point was on the trace of Vedi Fault. On the contrary, due to the existing researches, Vedi Fault is a geology fault, and not an active fault. Therefore, the one possibility of the activity near Nor Ughi point in Vedi Fault was thought that Vedi Fault might move as a secondary action due to the Yerevan Fault activity. Though a secondary fault activity, since it was found near Yerevan Fault, it was judged as possible and proposed a trench survey at Yerevan Fault, and realized in 2011 project.

(1) Trench Survey at Yerevan Fault

As mentioned above, the trench survey at Yerevan Fault initially was thought to be difficult, but the following possibilities were estimated;

1) a portion of the fault may appear near the ground surface

2) though a fault will not be confirmed, some traces of deformation or liquefaction trace may be found

3) activity duration may be estimated from the survey at secondary fault like Nor Ughi point 1-1

As shown in Figure 3.7-35, low scarp can be confirmed at northern and north-eastern edge of Ararat Basin. Therefore, on site investigation was conducted around the estimated scarp to find appropriate trench survey points on Yerevan Fault. As the results, 3 trenches were conducted at Metsamor (2 points), and at Nor Ughi (1 point) on Yerevan Fault (Figure 3.7-35, Figure 3.7-36 and Figure 3.7-37). However, neither fault of Yerevan Fault nor traces of deformation and liquefaction was confirmed by these trenches. According to the satellite imageries, low scarp was clear, but it was gentle slope on site. It showed trench survey was difficult. Further, since due to agriculture activities, the ground surface was remarkably deformed, the location of estimated low scarp was difficult to find out.

Even though trench survey across Yerevan Fault could not find a fault, it is one possibility that Yerevan Fault might generate earthquake with magnitude less than 7, because most of earthquakes in the world with magnitude less than 7 often remain no traces at ground surface.

(2) Trench Survey at Nor Ughi 1-2 Point

Since the fault found at Nor Ughi 1-1 point deforms unconsolidated soil layer, it is estimated a clear active fault. However, due to no dating test in the last year, there was a question that Vedi Fault is old and not active. For this reason, the trench survey at Nor Ughi 1-2 site across Vedi Fault was conducted for the purpose of dating (Figure 3.7-38, Figure 3.7-39 and Figure 3.7-40). 7 samples for dating were gotten at Nor Ughi 1-2 point trench, and the results of dating test are shown in the photo of the walls The sand and gravel layers in the trench show the ages between AD70 to 1450. Thus,

Vedi Fault is confirmed as active and the found activity will have a possibility of the 893 Dvin Earthquake.

Unfortunately, since this area is dry climate, samples of carbide or organic materials for good dating test are somewhat difficult. Organic soils in gravel layer were used for the test this time. As the quality of samples was not so good, it is preferable to check by more trenches with dating tests of ^{14}C, or other dating method like OSL method. And OSL method is recommended because it can be conducted in Armenia.

(3) Interpretation of the result at Nor Ughi Site

The fault found at Nor Ughi 1-2 site is corresponded to the one at Nor Ughi 1-1 site. However, according to the existing literatures, Vedi Fault is not active. Also, the trace of it runs through the valley of Vedi and going for eastern mountains, which is different from the trace of Yerevan Fault.

The fact that a portion of Vedi Fault is active and it might generate an earthquake will be estimated by either the next two;

1） Vedi Fault is not geology fault, but active fault
2） Vedi Fault is geology fault and move as a secondary

For the verification of 2), it is necessary to confirm the existence of primary fault. Though still there are various unknown factors, it is a quite remarkable outcome to find out an active fault at Nor Ughi of Vedi Fault by the trench survey.

The survey in this project showed that since Yerevan Fault is blind, trench survey cannot identify the fault. Therefore, in order to identify Yerevan Fault, it is recommended to adopt physical prospecting such as seismic reflection method in the future.
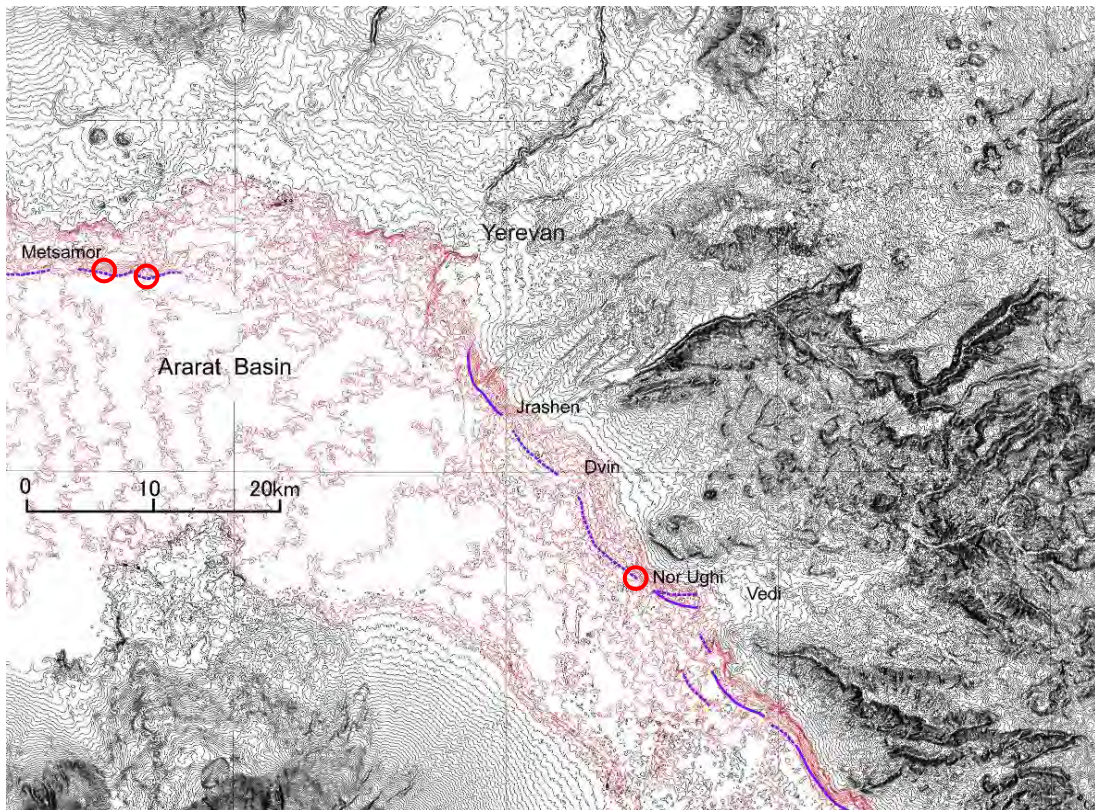
Figure 3.7-35   Estimated low scarp by satellite images along north edge to southeast edge of Ararat Basin (purple line)   3 trenches, 2 at Metsamor, 1 at Nor Ughi across Yerevan Fault were conducted (red circles).
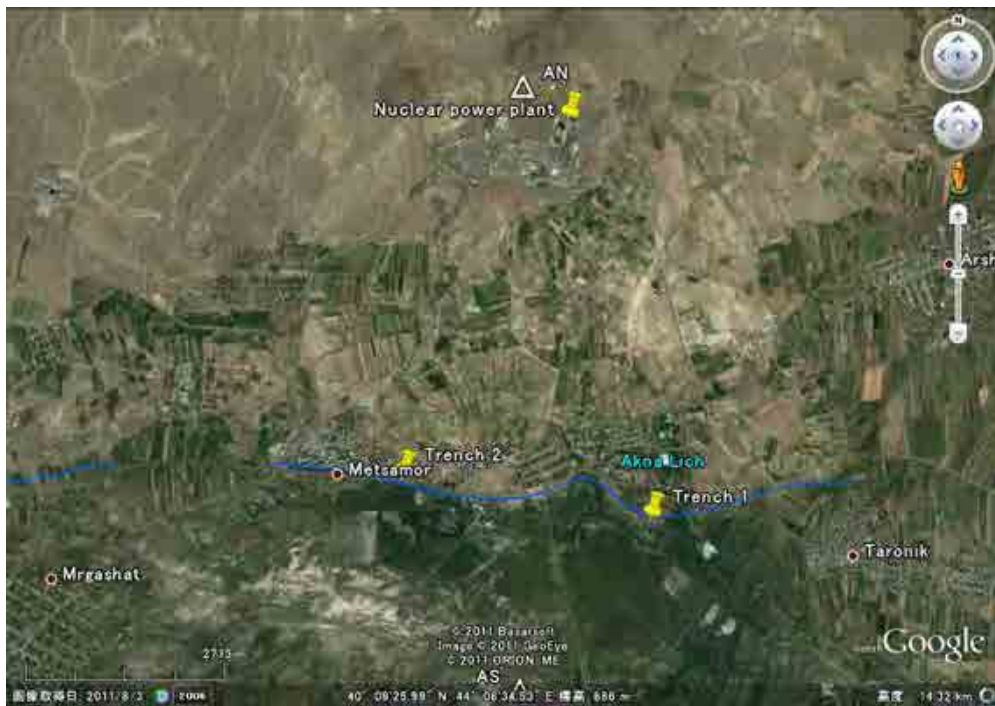

Figure 3.7-36   Trenches at Metsamor site. Blue line is estimated Yerevan Fault. Two trenches were conducted, but Yerevan Fault could not be identified.
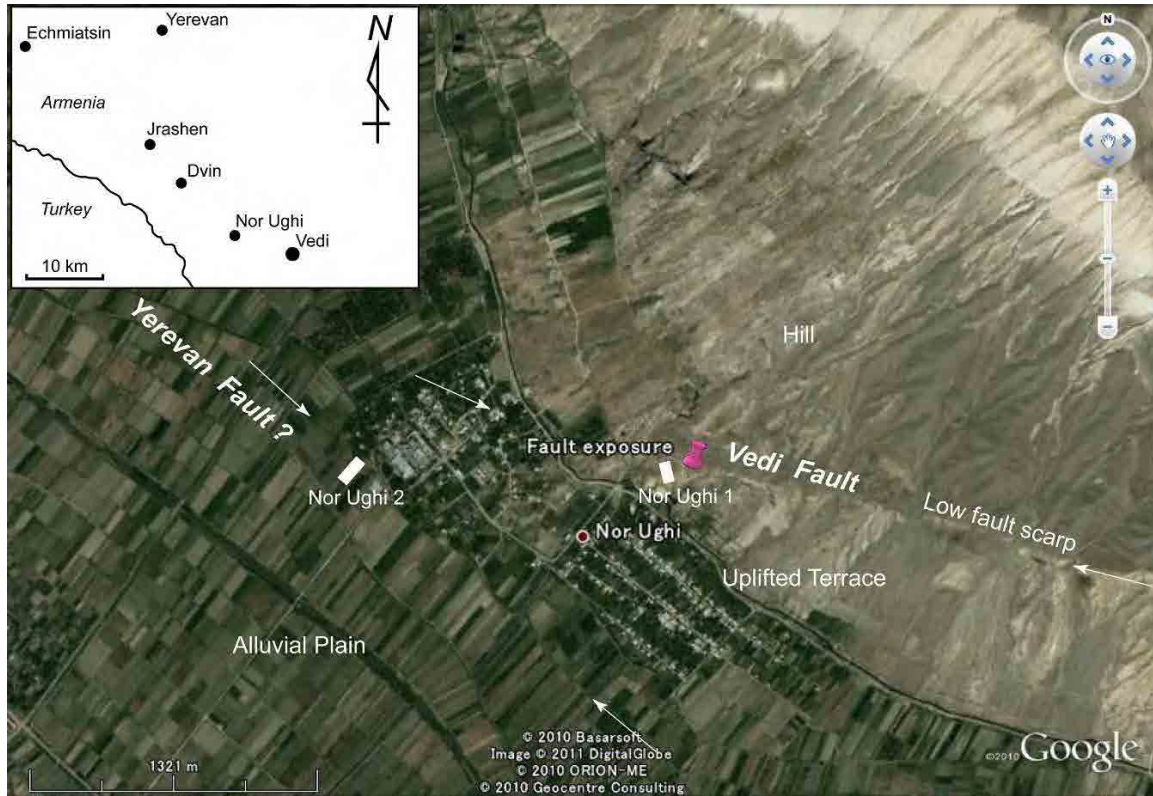
Figure 3.7-37   Location of trenches at Nor Ughi site.   Two trenches at Nor Ughi 1 (Vedi Fault). And one trench at Nor Ughi 2 (Yerevan Fault) where Yerevan Fault could not be identified.
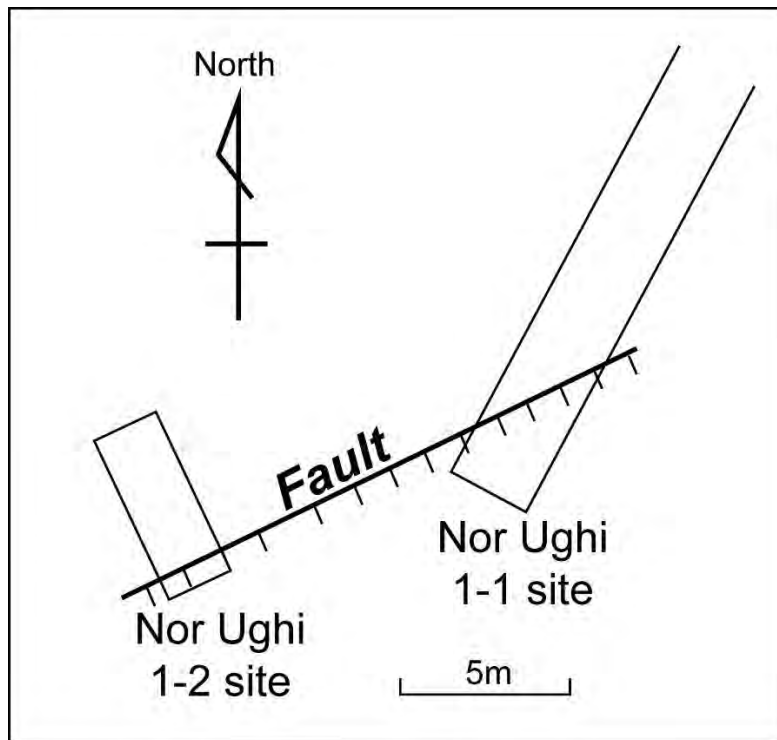

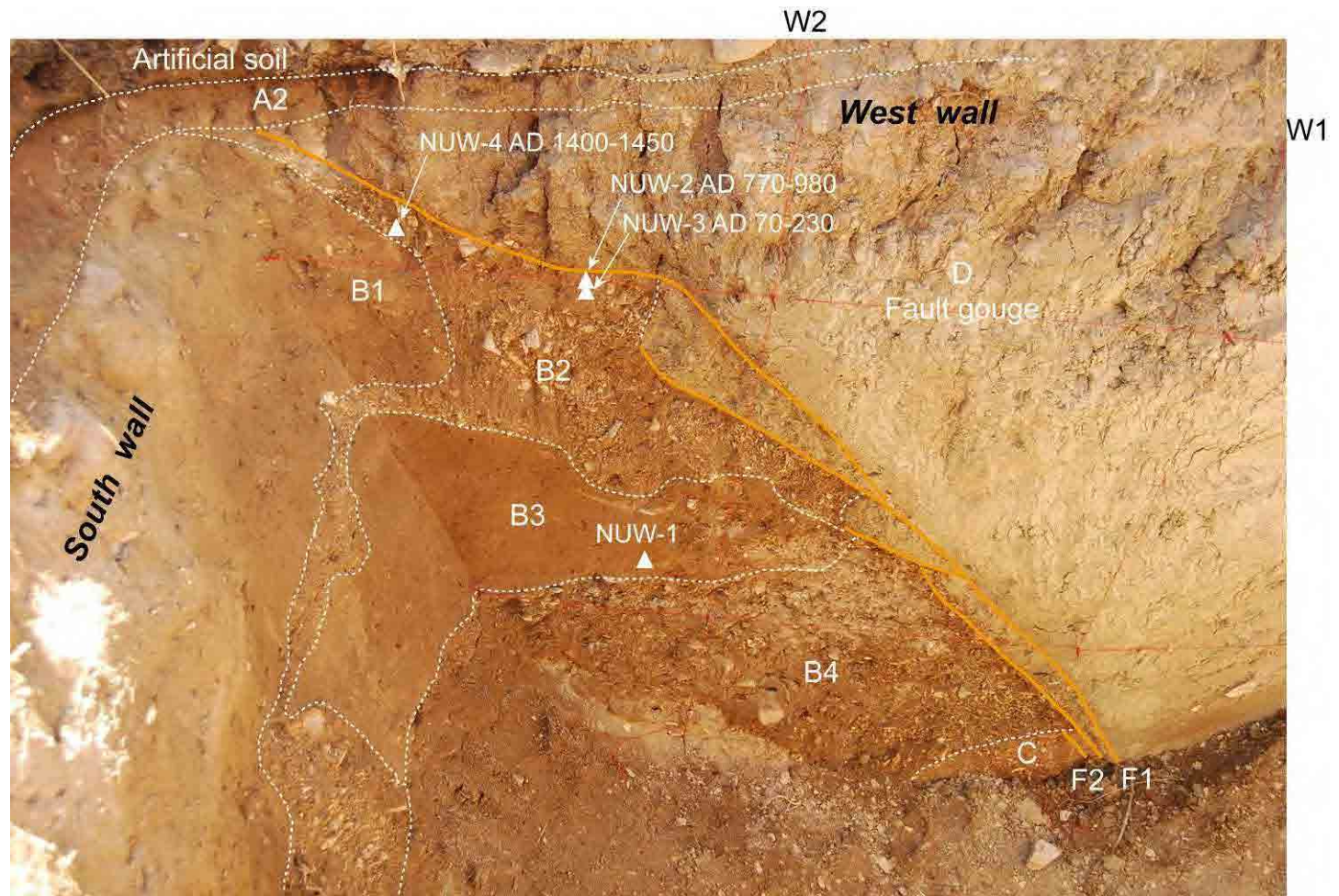Figure 3.7-38   Location of two trenches at Nor Ughi 1-1 and 1-2 sites

Figure 3.7-39　A photo of west wall at trench of Nor Ughi 1-2 point. A Tertiary layer overlies unconsolidated gravel layers of B1 to B4 and C. F1 fault moved after AD 70-980 (NUW-2) or after AD1400-1450 (NUW-4).

Figure 3.7-40　A photo of east wall at the trench of Nor Ughi 1-2 point. The fault F1, covered by layers of A1 and A2, is estimated to move between BC 810-590 and AD 1160-1270.

References:

Aslanyan, A. T., 1954, Deep fault near Yerevan City. Volume of contribution summaries of the 6th Science and Technology Conference of the Transcaucasian High Technological University Professors and Lecturers (in Russian)

Aslanyan, A. T., 1958. Regional geology of Armenia, HaiPetHrat, Yerevan (in Russian)

Gabriyelyan, A. A., 1959, Main issues of the geotectonics in Armenia. Publishing House of the AS of the Armenian SSR, Yerevan (in Russian)

Gabriyelyan, A. A., O. A. Sargsyan, and G. P. Simonyan, 1981, Seismotectonics of the Armenian SSR. Publishing House of the Yerevan State University, Yerevan (in Russian)

Gilbert, G. K., 1890, Lake Bonneville. U.S. Geol. Survey Monograph 1.

Karakhanian, A.S., V.G. Trifonov, H. Philip, A. Avagyan, K. Hessami, F. Jamali, M.S. Bayraktutan, H. Bagdassarian, S. Arakelian, V. Davtian, and A. Adilkhanyan, 2004, Active faulting and natural hazards in Armenia, eastern Turkey and northwestern Iran. Tectonophysics, 380, 189-219.

McCalpin J. P., edited, 1996, Paleoseismology; Academic Press New York p.588.

Nelson, A. R., 1992, Lithofacies analysis of colluvial sediments- an aid in interpreting the recent history of Quaternary normal faults in the Basin and Range province, western United States. *J. Sediment, Pet.*, 62**,** 607-621.

Philip, H., E. Rogozhin, A. Cisternas, J.C. Bousguet, A. Borisov, A.S. Karakhanian, 1992, The Armenian earthquake of 1988 December 7: faulting and folding, neotectonics and paleo – seismicity. Geophys. Int. J., 110, 141-158.

Philip, H., A. Avagyan, A. Karakhanian, J.-F. Ritz, and S. Rebai, 2001, Slip rates and recurrence intervals of strong earthquakes along the Pambak-Sevan-Sunik fault (Armenia). Tectonophysics, 343 (3-4), 205-232.

Reimer, P.J., Baillie, M.G.L., Bard, E., Bayliss, A., Beck, J.W., Bertrand, C.J.H., Blackwell, P.G., Buck, C.E., Burr, G.S., Cutler, K.B., Damon, P.E., Edwards, R.L., Fairbanks, R.G., Friedrich, M., Guilderson, T.P., Hogg, A.G., Hughen, K.A., Kromer, B., McCormac, G., Manning, S., Bronk Ramsey, C., Reimer, R.W., Remmele, S., Southon, J.R., Stuiver, M., Talamo, S., Taylor, F.W., van der Plicht, J., Weyhenmeyer, C.E., 2004. IntCal04 terrestrial radiocarbon age calibration, 0-26 cal kyr BP. Radiocarbon 46, 1029-1058.

Tovmasyan, A. K., 2008, Focal Mechanisms of Yerevan Earthquakes. The modern main issues of Geology and Geography, 297-305.

Wang, Y. and Q. Deng, edited, 1988, Active fault system around Ordos Massif. The Research Group on "Active Fault System around Ordos Massif", Beijing: State Seismology Bureau, 335p.

Wells, D. L. and K. J. Coppersmith (1994) New Empirical Relationships among Magnitude, Rupture Length, Rupture Width, Rupture Area, and Surface Displacement. *Bull. Seismol. Soc. Am.*, **84**, 974-1002.

Xiano, H. and J. Suppe, 1992, Origin of rollover. American Association of Petroleum Geologists Bull. **76**, 509-529.

Georisk report

Report on the Garni Fault,20p.

Report on the analysis of strong historical earthquakes located near to the ANPP (Armenian Nuclear Power Plant), 174-268.

Report on the Yerevan Fault, 43p.